ResQ-IOS: An iterative optimization-based simulation framework for quantifying the resilience of interdependent critical infrastructure systems to natural hazards

Journal Article

Author(s):
Hafeznia, Hamed; Stojadinovic, Bozidar (ID)

ELSEVIER

ResQ-IOS: An iterative optimization-based simulation framework for quantifying the resilience of interdependent critical infrastructure systems to natural hazards

Hamed Hafeznia [a,b,*], Božidar Stojadinović [a,b]

[a] Institute of Structural Engineering, Department of Civil, Environmental and Geomatic Engineering, ETH Zürich, 8093 Zurich, Switzerland
[b] Singapore-ETH Centre, Future Resilient Systems, CREATE Campus, 1 CREATE Way, #06-01 CREATE Tower, Singapore 138602, Singapore

HIGHLIGHTS

- ResQ-IOS can quantify interdependent critical infrastructure systems' resilience.
- This framework can consider partial failure and functionality level for components.
- ResQ-IOS allows for components' nonlinear properties and time-dependent demands.
- ResQ-IOS can be utilized for the resilience-oriented development of communities.
- Resilience of interdependent infrastructure systems in Shelby County is assessed.

ARTICLE INFO

ABSTRACT

Critical Infrastructure Systems are highly complex and interdependent. Growing complexity and interdependency between infrastructure systems and frequent exposure to extreme events have inevitably increased the probability of cascading failures and the prolonged lack of serviceability in urban communities, especially so for energy systems. The resilience analysis of interdependent infrastructure systems against natural hazards provides stakeholders with a comprehensive outlook on recovery strategies to minimize the damage costs and losses caused by extreme events. This paper introduces the ResQ-IOS, a Resilience Quantification Iterative Optimization-based Simulation (IOS) framework for quantifying the resilience of interdependent infrastructure systems to natural hazards with the capability of considering the real-world conditions for the status of infrastructure systems' components. The ResQ-IOS framework consists of five modules: risk assessment, simulation, optimization, database, and controller. To evaluate the capabilities of this framework, the seismic resilience of interdependent energy infrastructure networks (power, natural gas, and water) in Shelby County (TN), USA, was assessed. The results of the resilience analysis of the case study suggest that the water network is the best candidate for implementing pre-disaster Resilience Enhancement Measures (REMs), like increasing the supply capacity. Due to the controlling role of the power network in the community's recovery process, it is recommended that post-disaster REMs, such as increasing the number of Repair and Maintenance (R&M) teams, should be applied to the power network to speed up the restoration of failed components in that network and consequently, shorten the recovery duration of the community. The ResQ-IOS can be employed as a useful computational tool for planning the resilience-oriented sustainable development of urban communities by, for example, deploying Renewable Energy (RE)-based strategies to enhance their disaster resilience.

1. Introduction

Critical Infrastructure Systems (CISs) play a vital role in regional socioeconomic development by providing the essential resources, including different types of energy, water, transportation and communication [1–3]. A disruption in the performance of an energy infrastructure system usually results in the inoperability of other

---

Nomenclature

Abbreviations

IOS	Iterative Optimization-based Simulation
CISs	Critical Infrastructure Systems
EISs	Energy Infrastructure Systems
OS	Optimization-Simulation
MILP	Mixed-Integer Linear Programming
ALR	Accumulated Loss of Resilience
SoCIS-ALR	joint Accumulated Loss of Resilience (for a system of CISs)
R&M	Repair and Maintenance
GTPP	Gas Turbine Power Plant
CCPP	Combined-Cycle Power Plant
PGS	Power Gate Station
LNGT	Liquefied Natural Gas Terminal
NGPP	Natural Gas Processing Plant
NGGS	Natural Gas Gate Station
ESS	Electric Substation
BSU	Building Stock Unit
NGCS	Natural Gas Compressor Station
WSF	Water Supply Facility
WPS	Water Pump Station
WST	Water Storage Tank

Indices and sets

i	Index of critical infrastructure systems
CIS	Set of critical infrastructure systems
s	Index of nodes in the critical infrastructure system
SN^i	Set of nodes in the critical infrastructure system i
f	Index of facilities in the critical infrastructure system
SF^i	Set of facilities in the critical infrastructure system i
m	Index of nodes in the power network
n	Index of nodes in the natural gas network
j	Index of nodes in the water network
p	Index of powerlines in the power network
q	Index of pipelines in the natural gas network
l	Index of pipelines in the water network
NE	Set of nodes in the power network
NG	Set of nodes in the natural gas network
NW	Set of nodes in the water network
LE	Set of power lines in the power network
LG	Set of pipelines in the natural gas network
LW	Set of pipelines in the water network
t	Index of time steps
T	Set of total time steps between t_E and t_R
f_e	Index of facilities in the power network
FE	Set of facilities in the power network
f_g	Index of facilities in the natural gas network
FG	Set of facilities in the natural gas network
f_w	Index of facilities in the water network
FW	Set of facilities in the water network
$IGtE$	Set of interdependent nodes coupled between the natural gas and power networks (Gas to Power)
$IWtE$	Set of interdependent nodes coupled between the water and power networks (Water to Power)
$IEtG$	Set of interdependent nodes coupled between the power and natural gas networks (Power to Gas)
$IEtW$	Set of interdependent nodes coupled between the power and water networks (Power to Water)

Variables

R^i	Accumulated loss of resilience for an individual infrastructure system over the disruption period
R^{SoCIS}	Accumulated loss of resilience for interdependent infrastructure systems over the disruption period
R_t^{SoCIS}	Accumulated loss of resilience for interdependent infrastructure systems at time t
P_{pre}^i	Pre-disruption performance of an individual infrastructure system
P_{post}^i	Post-disruption performance of an individual infrastructure system
$C_{sys}^{pre,i}$	Total consumption of the service in the infrastructure network i before disruption
$D_{sys}^{pre,i}$	Total demand for the service in the infrastructure network i before disruption
$C_{sys}^{post,i}$	Total consumption of the service in the infrastructure network i after disruption
$D_{sys}^{post,i}$	Total demand for the service in the infrastructure network i after disruption
$E_{G,t}^m$	Total electric power generation at electric node m at time t
$E_{C,t}^m$	Total electric power consumption at electric node m at time t
e_t^p	Electric power flow through the powerline p at time t
$E_{G,t}^{GTPP,m}$	Electric power generation of GTPP at electric node m at time t
$E_{G,t}^{CCPP,m}$	Electric power generation of CCPP at electric node m at time t
$E_{G,t}^{PGS,m}$	Electric power imported by PGS at electric node m at time t
$E_{C,t}^{GTPP,m}$	Electric power consumption for GTPP at electric node m at time t
$E_{C,t}^{CCPP,m}$	Electric power consumption for CCPP at electric node m at time t
$E_{C,t}^{ESS,m}$	Electric power consumption for ESS at electric node m at time t
$E_{C,t}^{NGPP,m}$	Electric power consumption for NGPP at electric node m at time t
$E_{C,t}^{LNGT,m}$	Electric power consumption for LNGT at electric node m at time t
$E_{C,t}^{NGCS,m}$	Electric power consumption for NGCS at electric node m at time t
$E_{C,t}^{WSF,m}$	Electric power consumption for WSF at electric node m at time t
$E_{C,t}^{WPS,m}$	Electric power consumption for WPS at electric node m at time t
$E_{C,t}^H$	Electric power consumption for BSU H located in the service area of electric node m at time t
$z_{E,t}^p$	Binary variable indicating the operating state of powerline p at time t
$x_{E,t}^m$	Binary variable indicating the operating state of electric node m at time t
g_t^q	Natural gas flow through the pipeline q at time t
$G_{G,t}^n$	Total natural gas production at gas node n at time t
$G_{C,t}^n$	Total natural gas consumption at gas node n at time t
$G_{G,t}^{LNGT,n}$	Natural gas production of LNGT at gas node n at time t
$G_{G,t}^{NGPP,n}$	Natural gas production of NGPP at gas node n at time t
$G_{G,t}^{NGGS,n}$	Natural gas imported by NGGS at gas node n at time t
$G_{C,t}^{GTPP,n}$	Natural gas consumption for GTPP at gas node n at time t
$G_{C,t}^{CCPP,n}$	Natural gas consumption for CCPP at gas node n at time t
$G_{C,t}^{NGPP,n}$	Natural gas consumption for NGPP at gas node n at time t
$G_{C,t}^{LNGT,n}$	Natural gas consumption for LNGT at gas node n at time t
$G_{C,t}^{NGCS,n}$	Natural gas consumption for NGCS at gas node n at time t

$G_{C,t}^{H}$ — Natural gas consumption for BSU H located in the service area of gas node n at time t

$z_{G,t}^{q}$ — Binary variable indicating the operating state of gas pipeline q at time t

$x_{G,t}^{n}$ — Binary variable indicating the operating state of gas node n at time t

w_{t}^{l} — Water flow through the pipeline l at time t

$W_{G,t}^{j}$ — Total water supply at water node j at time t

$W_{C,t}^{j}$ — Total water consumption at water node j at time t

$W_{G,t}^{WSF,j}$ — Water supply by WSF at water node j at time t

$W_{G,t}^{WST,j}$ — Water supply by WST at water node j at time t

$W_{C,t}^{CCPP,j}$ — Water consumption for CCPP at water node j at time t

$W_{C,t}^{H}$ — Water consumption for BSU H located in the service area of water node j at time t

$z_{W,t}^{l}$ — Binary variable indicating the operating state of water pipeline l at time t

$x_{W,t}^{j}$ — Binary variable indicating the operating state of water node j at time t

$\varphi_{E,t}^{GTPP,m}$ — Binary variable indicating the operating state of GTPP at electric node m at time t

$\theta_{t}^{GTPP,n}$ — Binary variable indicating the operating state of the interdependency link from gas node n to GTPP at electric node m at time t

$\delta_{t}^{GTPP,n}$ — Binary variable indicating the operating state of gas supply system for GTPP at gas node n at time t

$\varphi_{E,t}^{CCPP,m}$ — Binary variable indicating the operating state of CCPP at electric node m at time t

$\theta_{t}^{CCPP,n}$ — Binary variable indicating the operating state of the interdependency link from gas node n to CCPP at electric node m at time t

$\delta_{t}^{CCPP,n}$ — Binary variable indicating the operating state of gas supply system for CCPP at gas node n at time t

$\sigma_{t}^{CCPP,j}$ — Binary variable indicating the operating state of the interdependency link from water node j to CCPP at electric node m at time t

$\gamma_{t}^{CCPP,j}$ — Binary variable indicating the operating state of water supply system for CCPP at water node j at time t

$\varphi_{E,t}^{PGS,m}$ — Binary variable indicating the operating state of PGS at electric node m at time t

$\varphi_{E,t}^{ESS,m}$ — Binary variable indicating the operating state of ESS at electric node m at time t

$\varphi_{G,t}^{LNGT,n}$ — Binary variable indicating the operating state of LNGT at gas node n at time t

$\alpha_{t}^{LNGT,m}$ — Binary variable indicating the operating state of the interdependency link from electric node m to LNGT at gas node n at time t

$\pi_{t}^{LNGT,m}$ — Binary variable indicating the operating state of power supply system for LNGT at electric node m at time t

$\varphi_{G,t}^{NGPP,n}$ — Binary variable indicating the operating state of NGPP at gas node n at time t

$\alpha_{t}^{NGPP,m}$ — Binary variable indicating the operating state of the interdependency link from electric node m to NGPP at gas node n at time t

$\pi_{t}^{NGPP,m}$ — Binary variable indicating the operating state of power supply system for NGPP at electric node m at time t

$\varphi_{G,t}^{NGGS,n}$ — Binary variable indicating the operating state of NGGS at gas node n at time t

$\varphi_{G,t}^{NGCS,n}$ — Binary variable indicating the operating state of NGCS at gas node n at time t

$\alpha_{t}^{NGCS,m}$ — Binary variable indicating the operating state of the interdependency link from electric node m to NGCS at gas node n at time t

$\pi_{t}^{NGCS,m}$ — Binary variable indicating the operating state of power supply system for NGCS at electric node m at time t

$\varphi_{W,t}^{WSF,j}$ — Binary variable indicating the operating state of WSF at water node j at time t

$\beta_{t}^{WSF,m}$ — Binary variable indicating the operating state of the interdependency link from electric node m to WSF at water node j at time t

$\pi_{t}^{WSF,m}$ — Binary variable indicating the operating state of power supply system for WSF at electric node m at time t

$\varphi_{W,t}^{WPS,j}$ — Binary variable indicating the operating state of WPS at water node j at time t

$\beta_{t}^{WPS,m}$ — Binary variable indicating the operating state of the interdependency link from electric node m to WPS at water node j at time t

$\pi_{t}^{WPS,m}$ — Binary variable indicating the operating state of power supply system for WPS at electric node m at time t

$\varphi_{W,t}^{WST,j}$ — Binary variable indicating the operating state of WST at water node j at time t

Parameters

t_{E} — Beginning time of system disruption

t_{R} — Ending time of the recovery process

ω_{i} — Pre-determined weights related to the relative importance of infrastructure systems

$S(link)$ — Start node of the link

$T(link)$ — Terminal node of the link

e_{cap}^{p} — Flow capacity of the powerline p

g_{cap}^{q} — Flow capacity of the gas pipeline q

w_{cap}^{l} — Flow capacity of the water pipeline l

$\tau_{E,t}^{m}$ — Binary parameter indicating whether the recovery process started at electric node m at time t

$\tau_{G,t}^{n}$ — Binary parameter indicating whether the recovery process started at gas node n at time t

$\tau_{W,t}^{j}$ — Binary parameter indicating whether the recovery process started at water node j at time t

$S_{E,t}^{GTPP,m}$ — Electric power generation capacity of GTPP at electric node m at time t

$D_{E,t}^{GTPP,m}$ — Electric power demand of GTPP at electric node m at time t

$D_{G,t}^{GTPP,n}$ — Natural gas demand of GTPP at gas node n at time t

$S_{E,t}^{CCPP,m}$ — Electric power generation capacity of CCPP at electric node m at time t

$D_{E,t}^{CCPP,m}$ — Electric power demand of CCPP at electric node m at time t

$D_{G,t}^{CCPP,n}$ — Natural gas demand of CCPP at gas node n at time t

$D_{W,t}^{CCPP,j}$ — Water demand of CCPP at water node j at time t

$S_{E,t}^{PGS,m}$ — Electric power import capacity of PGS at electric node m at time t

$D_{E,t}^{ESS,m}$ — Electric power demand of ESS at electric node m at time t

$D_{E,t}^{H}$ — Electric power demand of BSU H located in the service area of electric node m at time t

$S_{G,t}^{LNGT,n}$ — Natural gas production capacity of LNGT at gas node n at time t

$D_{G,t}^{LNGT,n}$ — Natural gas demand of LNGT at gas node n at time t

$D_{E,t}^{LNGT,m}$ — Electric power demand of LNGT at electric node m at time t

$S_{G,t}^{NGPP,n}$ — Natural gas production capacity of NGPP at gas node n at time t

$D_{G,t}^{NGPP,n}$ — Natural gas demand of NGPP at gas node n at time t

$D_{E,t}^{NGPP,m}$	Electric power demand of NGPP at electric node m at time t	$D_{E,t}^{WPS,m}$	Electric power demand of WPS at electric node m at time t
$S_{G,t}^{NGGS,n}$	Natural gas import capacity of NGGS at gas node n at time t	$D_{W,t}^{H}$	Water demand of BSU H located in the service area of water node j at time t
$D_{G,t}^{NGCS,n}$	Natural gas demand of NGCS at gas node n at time t	$\mu_{E,t}^{p}$	Binary parameter indicating whether the powerline p is restored at time t
$D_{E,t}^{NGCS,m}$	Electric power demand of NGCS at electric node m at time t		
$D_{G,t}^{H}$	Natural gas demand of BSU H located in the service area of gas node n at time t	$\mu_{G,t}^{q}$	Binary parameter indicating whether the gas pipeline q is restored at time t
$S_{W,t}^{WSF,j}$	Water supply capacity of WSF at water node j at time t	$\mu_{W,t}^{l}$	Binary parameter indicating whether the water pipeline l is restored at time t
$S_{W,t}^{WST,j}$	Water supply capacity of WST at water node j at time t		
$D_{E,t}^{WSF,m}$	Electric power demand of WSF at electric node m at time t		

interdependent civil infrastructure systems, such as water, communication and transportation networks. Thus, regional governments and community stakeholders are concerned about the stable, reliable, and sustainable supply of energy resources to maintain their communities' economic growth and social development [4,5].

Nowadays, Energy Infrastructure Systems (EISs) are highly interdependent and interconnected [6–8]. Due to interdependencies between the EISs and other civil infrastructure systems, a malfunction in the performance of energy infrastructure systems, consisting of many components, may significantly impact the economic sectors of the society [8–13]. CISs are frequently exposed to the occurrence of disruptive events, including man-made threats and natural hazards, such as earthquakes, hurricanes, floods, and windstorms [10,14–16]. To minimize the damage costs and losses caused by extreme events to critical infrastructure systems, resilience enhancement has been adopted as a key strategy by government agencies, infrastructure managers, and stakeholders [3,8,17–24].

The definition of resilience varies as research objectives, methodology, and case studies change. In other words, there is no general agreement on the resilience definition of energy systems, indicators, and quantitative metrics [3]. This study defines an infrastructure system's resilience as the ability of that system to minimize the consequences of the disturbance by anticipating, absorbing, adapting to, and recovering from the disruption.

Recently, Ahmadi et al. [3] have conducted a literature review on the system resilience modeling approaches. They categorized the resilience modeling approaches into three main groups: optimization, agent-based, and stochastic. The frequency of using other modeling approaches, such as simulation-based, system dynamic, and indicator-based modeling, is lower in the surveyed literature.

In optimization-based methods, the resilience assessment process for infrastructure systems is formulated as an optimization problem. The optimization problem aims to improve the post-disaster performance of the system. The optimal solution seeks to shorten the recovery process and reduce potential economic losses and system component damage. Kong et al. [8] provided a framework to optimize the resilience of interdependent infrastructure systems against natural disasters. This research work investigated some strategies to improve the resilience of infrastructure systems. Sang et al. [25] formulated a mixed-integer linear programming problem to find the optimal restoration sequence of damaged components in interdependent gas and electricity infrastructure systems. Liu et al. [26] developed a multi-objective optimization problem in a hierarchical framework to determine the optimal strategies for the resilience enhancement of interdependent power and natural gas infrastructure systems. Almoghathawi et al. [27] proposed a multi-objective optimization model to maximize the resilience of interdependent power and water networks while minimizing the cost of the recovery process. This model was formulated as a mixed-integer programming problem.

Dubaniowski and Heinimann [28] developed an agent-based Input-Output (IO) framework to model the interdependencies between the

infrastructure networks and the community, including the households and businesses. They applied the developed framework to an urban community in Singapore to assess resilience [29]. Sun et al. [30] presented an agent-based model for the recovery process of communities to appraise their seismic resilience. They also provided a resilience quantification framework for integrated civil infrastructure systems [31]. The studies [32,33] are examples of applying the agent-based modeling approach in resilience analysis.

The Monte Carlo simulation methods, widely applied to quantify the uncertainties in the resilience assessment of infrastructure systems, are typical examples of stochastic simulation-based methods. Some research studies [34–36] developed simulation-based methods to analyze the resilience of electricity networks under intense climatic conditions like hurricanes. Younesi et al. [15] provided a quantitative framework to assess the resilience of power networks against wide-area natural hazards. This framework applies Monte Carlo simulations to account for the uncertainties in some characteristics of natural hazards, including location, type, and severity level. Blagojevic et al. [37] presented a probability-based resilience quantification model for a virtual community. Many scenarios were simulated to calculate the community's resilience against earthquakes. The critical review of the literature on the resilience assessment of interdependent CISs identified the following research gaps:

1- The simulation-based and agent-based methods employed for resilience quantification do not necessarily guarantee the optimal distribution of resources and services throughout the infrastructure networks.

2- The initial operating state of components after disruption can be: completely failed, partially functional, or fully functional. In contrast, most of the research applying optimization models for resilience quantification considers a binary state for the operating condition of components after the disruption (failed or fully functional).

3- To reduce the computational burden, some papers consider a specific group of infrastructure systems' components for the resilience assessment, even though all components are subject to damage by natural hazards.

4- Some researchers apply a linear and deterministic approach for assessing infrastructure components' post-disaster damage state and functionality level. On the contrary, the Performance-Based Earthquake Engineering (PBEE) methodology uses a probabilistic approach to estimating the functionality loss of facilities after an earthquake.

5- In the recovery models developed for optimization-based frameworks, it is often assumed that each component is restored within a single time step of the resilience assessment period. This assumption is not realistic for short time steps and is not practical for large time steps.

6- Most of the reviewed research assumes that the demands posed by the components are constant and equal to their pre-disruption

demands during the entire resilience assessment process, whereas it is an unrealistic assumption. For example, demands for electric power, natural gas, and potable water in the network may decrease after the disaster that damages residential buildings since the residents of damaged buildings have to move to safe locations outside the network, or the power demand of a water pump station during the recovery process is proportional to the functionality level of that water pump station, and it may be less than the pre-disruption demand for power.

This paper presents a novel Resilience Quantification Iterative Optimization-based Simulation (ResQ-IOS) framework for modeling and analyzing the resilience of interdependent critical infrastructure systems against natural hazards. The ResQ-IOS framework takes advantage of both simulation-based and optimization-based approaches to address existing research gaps identified through the literature review on the resilience assessment of interdependent CISs. The following items are the main contributions:

1- The ResQ-IOS resilience quantification framework can determine the optimal flow of resources and services from and to each node in the network to maximize the resilience of interdependent infrastructure systems at each time step of the simulation and thus deliver a realistic resilience assessment, particularly for interacting diverse energy systems.
2- The proposed ResQ-IOS framework assumes that all components of the considered systems may be damaged during the disaster. This framework applies a probabilistic approach to estimate the damage state of the infrastructure systems' components. Also, the ResQ-IOS framework rates the functionality level of the components continuously, by using a fuzzy logic-based model.
3- In the ResQ-IOS framework, the required time for restoring the failed components depends on the failed component's damage state, which is a function of the characteristics of the hazard. Therefore, restoring damaged components may take several time steps in the resilience assessment period.
4- In the proposed ResQ-IOS framework, the demand for resources and services evolves in time after a disruptive event occurs. Thus, the demand for resources and services is a time-dependent function of the finicality level of the component during the resilience assessment period.
5- This ResQ-IOS makes it possible to consider the temporary loads that may be imposed on infrastructure networks during the recovery process. For example, if a water supply facility is out of service due to earthquake-induced damages, it does not mean that the demand of that facility for power is zero. Such a temporary load will be removed once the restoration process of that component is done.

The remainder of this research paper is organized as follows. Section 2 introduces the Iterative Optimization-based Simulation (IOS) framework and its modules for the resilience assessment of interdependent infrastructure networks. This section also presents the mathematical model of the optimization module for optimizing the resilience of interdependent CISs. Section 3 describes the case study involving the power, natural gas, and water systems in Shelby County, TN, USA, a realistic example of interdependent CISs. In Section 4, the resilience of the case study systems is quantified using the ResQ-IOS framework, and the sensitivity of the case study systems concerning a selected group of factors is examined. In Section 5, the conclusions of this study and the direction for future work are presented.

2. The iterative optimization-based simulation (IOS) framework for the resilience assessment of CISs

The capabilities of modern simulation tools to analyze complex systems' behavior by assessing their performance through creating 'what-if' scenarios makes simulation a robust methodology for solving real-world problems [38–40]. The simulation process computes system's performance measures for different model alternatives to evaluate the effects of model parameters on systems' behavior. However, an optimization process is needed to find the best configuration of the systems by exploring the systems' performance measures space generated by simulation. Integration of simulation and optimization is, therefore, a promising methodology for solving large and complex problems in the real-world environment [41].

Optimization approaches utilizing traditional mathematical optimization are readily applicable to small, deterministic, and less complex systems. As the system's size, uncertainty, and complexity increase, mathematical modeling may fail to find an optimal solution [42–46]. In contrast, hybrid Simulation-Optimization (SO) approaches can deal with the uncertainty and complexity of large-scale systems. Accordingly, SO models are more suitable for real-world stochastic and complex systems with sizable details and intricate relationships between their components [43,47,48]. Models using SO approaches can also consider the system's non-linear relationships, dynamic features, and qualitative aspects [46]. Significant progress in computational capacities has led to meaningful growth in applying SO models to various research fields, such as risk management, healthcare, and industrial engineering [41,49–52]. In the field of disaster resilience modeling, assessment and quantification of interacting civil infrastructures system, SO is particularly useful. This is particularly important when the involved systems have different disruption reaction times. For example, depending on the source of electric power (nuclear, natural gas, oil, coal, wind, water, solar), the time to stabilize the system after a disruption and restore its function may be very different.

The general structure of an Iterative Optimization-based Simulation (IOS) framework is illustrated in Fig. 1. According to this figure, an optimization solver is embedded into a simulation model in the structure of the proposed Iterative Optimization-based Simulation (IOS) framework. As shown in Fig. 1, the optimization solver is called repeatedly at each operational step of the IOS framework to optimize the simulated systems' state variables. Specifically, the simulation run is temporarily paused, and the state variables of the simulated system are transferred to the optimization solver as input to the analytical modeling of the system that is formulated as an optimization problem according to the current state of the simulated system. After the optimizer solves the mathematical model of the system and finds the solution, the framework updates the system's configuration according to the optimal solution and resumes the simulation run. This process is iterated between the optimization and simulation frequently until a pre-set stopping criterion is satisfied.

This paper introduces resilience quantification into an IOS framework by combining simulation and optimization. As shown in Fig. 2, the proposed Resilience Quantification Iterative Optimization-based Simulation (ResQ-IOS) framework for quantifying the resilience of interdependent CISs benefits from a modular workflow to establish logical relationships between the different sections of the framework. This IOS framework consists of five modules: risk assessment, simulation, optimization, database, and controller.

The block diagram of the process by which the ResQ-IOS models and quantifies the resilience of interdependent CISs is given in Fig. 3. The diagram comprises four major modules: Risk Assessment, Simulation, Optimization, and Controller. These four modules work together to evaluate the resilience of interdependent infrastructure systems. As depicted in Fig. 3, the first module that triggers the ResQ-IOS framework to operate is the risk assessment module. This module simulates the hazard and, accordingly, evaluates the vulnerability of the components of the infrastructure networks. Then, data related to the post-disaster status of the infrastructure networks as the output of the risk assessment module is conveyed to the database module. In the next step, the simulation module uses this data to simulate the functional recovery evolution of infrastructure networks' performance by tracing the
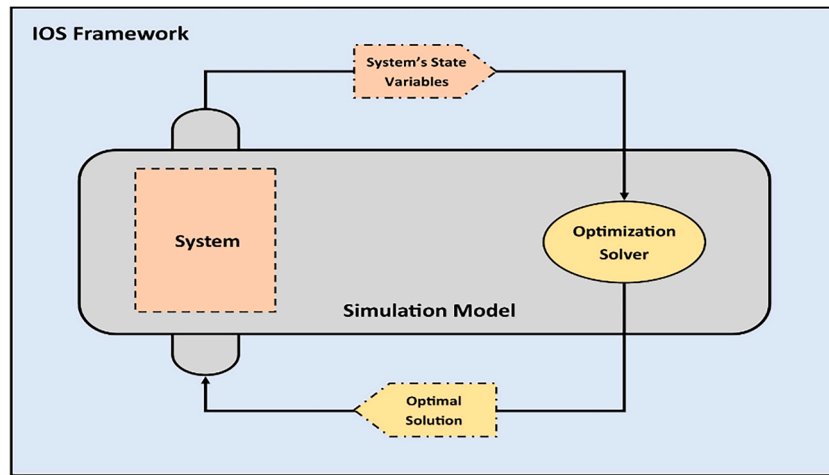
Fig. 1. An illustrative structure of the Iterative Optimization-based Simulation (IOS) framework.
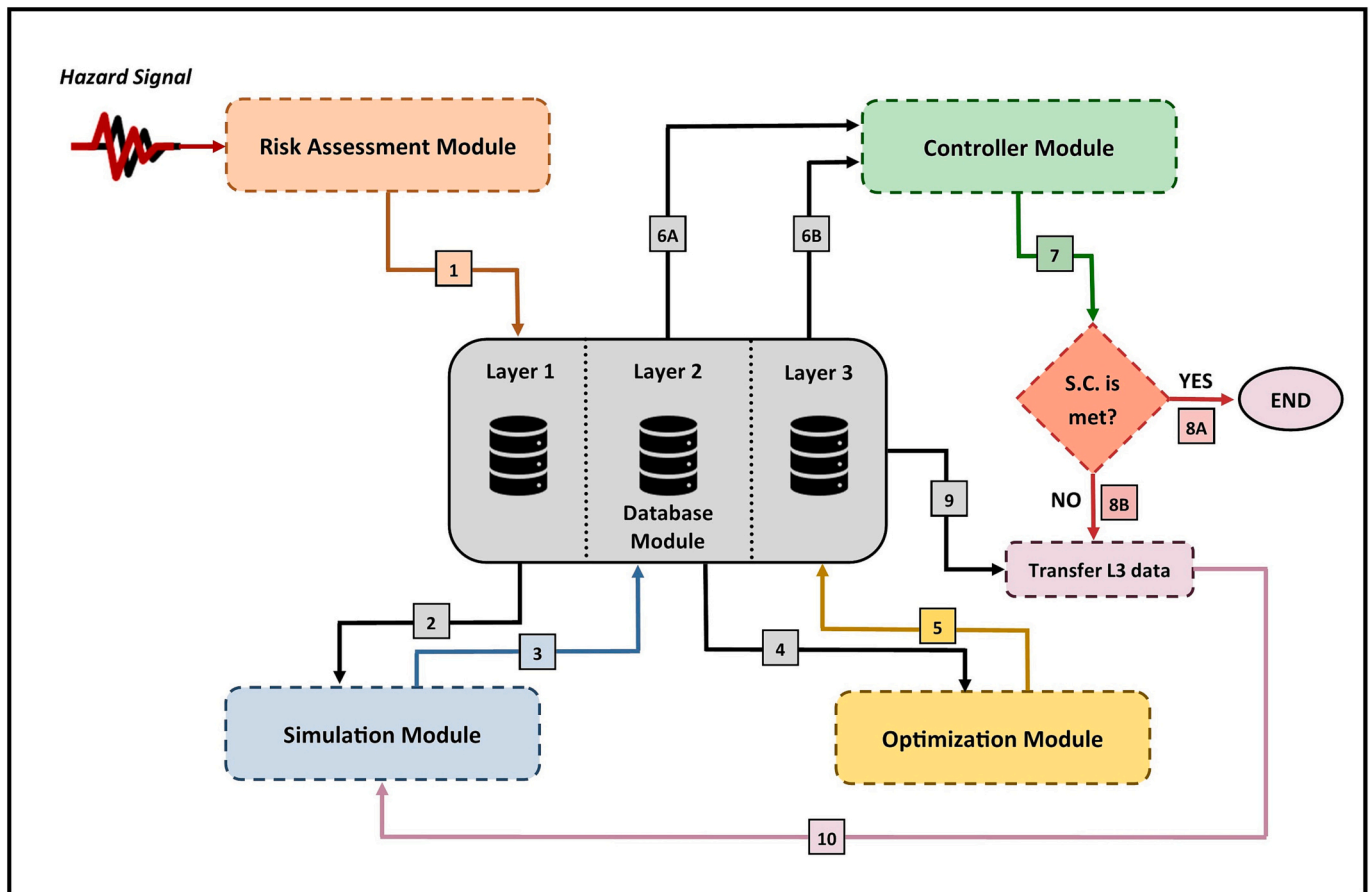

Fig. 2. The proposed ResQ-IOS framework for quantifying and optimizing the resilience of interdependent CISs.

functionality of components on both supply and demand sides according to their damage level and repair progress. This simulated data is populated to the database module and is utilized by the optimization module to maximize the post-disruption performance of the considered interdependent CISs. The optimization module solves a Mixed-Integer Linear Programming (MILP) problem to determine the optimal distribution of services and resources in the infrastructure networks. Then, the optimal solution is transferred to the database module. Concerning the infrastructure systems' optimal performance stored in the database, the simulation module reconfigures the supply and demand patterns in infrastructure networks. It then simulates the performance evolution of infrastructure networks for the next time step in the recovery process. This time-stepping Optimization-Simulation (OS) procedure is iterated between the simulation, database, and optimization modules. The controller module computes the loss of resilience for the infrastructure networks at each time step. The controller module ends the OS process when a set of pre-defined simulation stopping criteria is met.
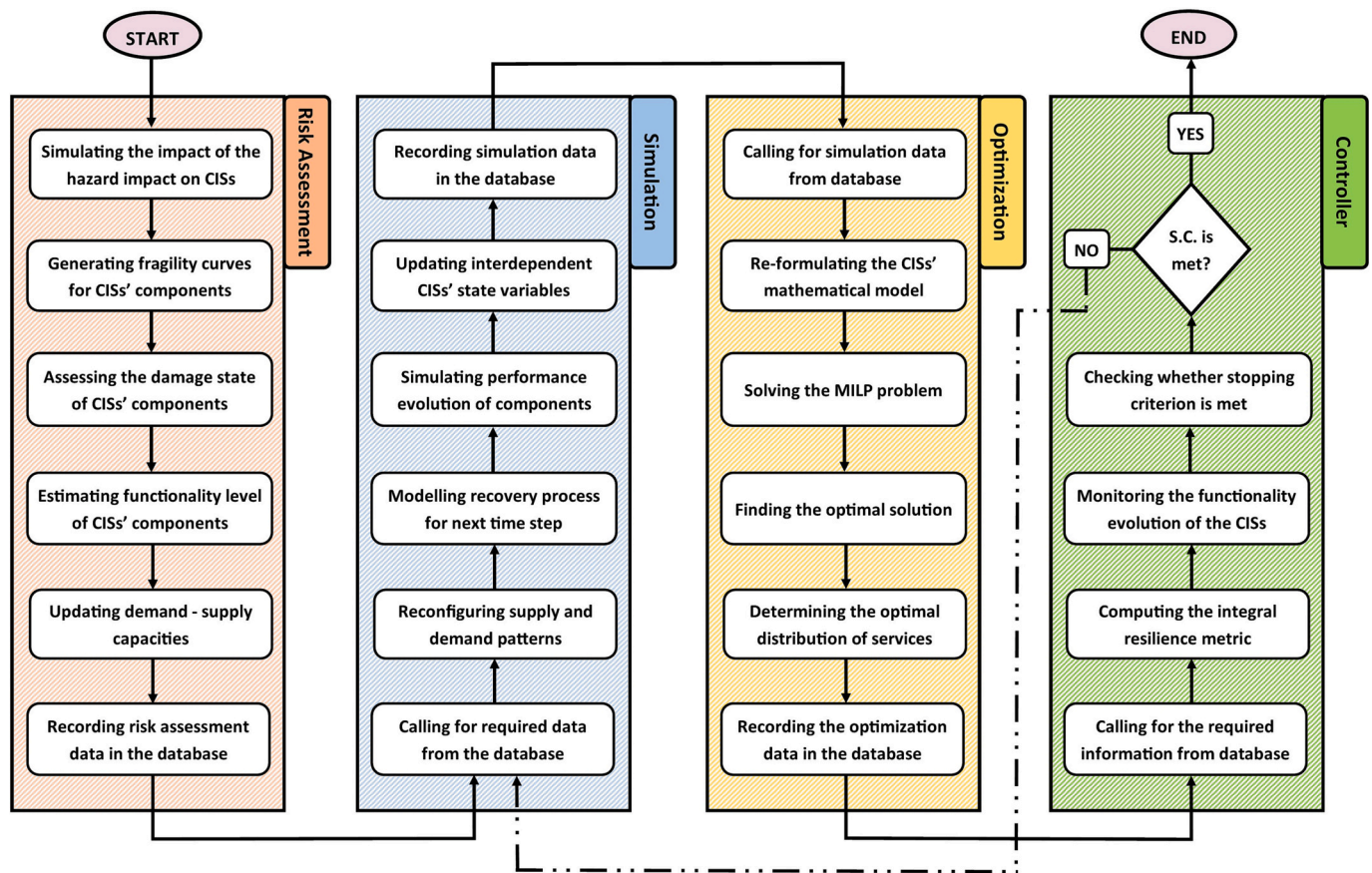
Fig. 3. The block diagram of the process used in the ResQ-IOS for modeling and quantifying the resilience of interdependent CISs.

2.1. Risk assessment module

The ResQ-IOS framework incorporates the risk assessment module to model how a hazard-induced disruption affects the functioning of a community and its interdependent infrastructure systems. The role of this module is to estimate the impact of the hazard on the performance of infrastructure systems' components. This module is the starter of workflow in the ResQ-IOS framework for the resilience assessment of interdependent CISs.

After the hazard-related disruption information is received, the risk assessment module begins to simulate the regional-scale impacts of the hazard on the infrastructure networks, considering the type and magnitude of the hazard. In this paper, the interdependent CISs' loss of functionality due to natural hazards is classified into two groups: direct and indirect functionality loss. Direct functionality loss is referred to the physical damage to the components of infrastructure networks. The physical damage includes structural and non-structural damage. For instance, the structural damage of a water pump station can be a partial collapse of the pump station building, and non-structural damage can be referred to as the equipment failure of the electrical power supply system in the pump station. Indirect functionality loss is referred to the inoperability of a component in the infrastructure system due to the malfunction in the performance of another infrastructure system that supplies the demand of that component in the dependent infrastructure system setting. For example, the water pump station, which remains intact after a natural hazard, may cease to operate if the electrical power network is damaged and not able to supply the pump station's demand. This type of functionality loss results from the interdependency between different infrastructure systems.

Taking an earthquake as an example of the hazard, the risk assessment module simulates the impact of the earthquake on the

infrastructure network by estimating intensity measures at the geographical location of the infrastructure networks' components. The earthquake intensity measures such as PGD, PGV, and PGA are calculated from the ground motion characteristics. To estimate the intensity measures at the locations of the systems' components, attenuation models that are the function of the earthquake magnitude and epicenter location are used. Then, the risk assessment module utilizes the seismic fragility curves of the infrastructure networks' components provided within component specification data. Considering the fragility curves and earthquake intensity measures at their location, the module assesses the components' vulnerability against the hazard and sets their initial post-disruption damage state. To this end, five damage states similar to the methodology of the FEMA-HAZUS Earthquake Model Technical Manual [53] are considered, namely, None, Slight, Moderate, Extensive, and Complete. The workflow of the risk assessment module is consistent with the Performance-Based Earthquake Engineering (PBEE) methodology developed by the Pacific Earthquake Engineering Research Center (PEER) [54]. Lastly, the risk assessment module sends information about the damage state of the components to the database module.

One of the strengths of the ResQ-IOS framework is that the resilience assessment process is formulated and implemented based on the time-dependent damage state of the components. Hence, this framework is capable of evaluating the resilience of interdependent CISs under the impact of multiple natural hazards (e.g., floods or high winds) as well as triggered natural hazard cascades.

2.2. Database module

In the ResQ-IOS framework, the role of the database module is to store the output data from the risk assessment, simulation, and optimization modules and provide the required data to those modules during

iterative resilience quantification (Fig. 2). In other words, the database module fulfills the module interface and data exchange roles. The database module consists of three layers. The first layer is allocated to store the output data sent by the risk assessment module. This data includes the damage state of the infrastructure networks' components caused by the hazard. The simulation module uses the data in this layer to trace the performance evolution of the CISs after the occurrence of the hazard.

The second layer of the database is dedicated to the output data of the simulation module, comprising the current functionality level of the CIS components and the current demand recovery of the consumers. The data of the second layer is fed to the optimization module. This data, which are the state variables of the community, is utilized to reformulate the MILP optimization problem that is representative of the community's mathematical model. As shown in Fig. 2, the optimal solution discovered by the optimization module is populated to the third layer of the database. The data stored in the third layer is then transferred to the simulation module to reconfigure the infrastructure networks and update the supply and demand patterns in the CISs and the community. The exchange of data between the ResQ-IOS framework's modules, as stated above, occurs until the controller module stops the time-stepping recovery OS process. The controller module takes the data from the second and third layers of the database to check whether the resilience quantification stopping criterion is satisfied.

2.3. Controller module

The tasks of the controller module are to monitor the functionality evolution of the CISs during the post-disruption recovery process, and to stop the time-stepping OS process once the stopping criteria are met. For these purposes, an integral resilience metric is defined to evaluate the joint recovery process of the interdependent CISs. The controller module computes this resilience metric in each the ResQ-IOS framework cycle. The module stops the resilience quantification framework when the resilience metric exceeds the pre-set threshold.

2.3.1. Resilience metric for interdependent CISs

There are a few candidates for a metric to quantify the joint disruption resilience of interdependent CISs. In some research studies [3,8,55–58], the resilience of an individual infrastructure system is calculated by the ratio of the area under the curve representing the time evolution of the actual performance of the infrastructure system with respect to the target performance of the system over the period starting from the occurrence of a disruptive event and ending when the recovery process is completed. Some researchers [59,60] quantified the resilience of an infrastructure system as the instantaneous difference between the actual and target system performance at certain time points during the recovery process. However, both groups of researchers use different indicators for infrastructure system performance.

In this paper, a resilience metric was defined to measure the resilience of an individual infrastructure system with respect to its pre-and post-disruption performance. The resilience of the infrastructure system following a disruptive event is quantified by tracking the evolution path of system performance after the disruption through time. This resilience metric adopted in this study is based on the Loss of Resilience metric proposed by Didier et al. [61]. An infrastructure system encounters a loss of resilience when it is not able to supply the amount of demand for its service. The resilience metric R^i used in this study is:

$$R^i = \int_{t_E}^{t_R} \left(P_{pre}^i(t) - P_{post}^i(t) \right) dt \tag{1}$$

where P_{pre}^i and P_{post}^i denote the infrastructure system's i pre and post-disruption performance, and t_E and t_R denote the times when the disruption occurs and the time when the recovery process ends, respectively. The instantaneous performance of the system $P^i(t)$ is the ratio of the instantaneous total consumption of its service (e.g., electrical power, water, etc.) $C_{sys}^i(t)$ and the instantaneous total demand for its service $D_{sys}^i(t)$ and measures its instantaneous Loss of Resilience (LR). By this definition, the performance of the system $P^i(t)$ is normalized and unitless, following [62], and takes values between 0 and 1. The
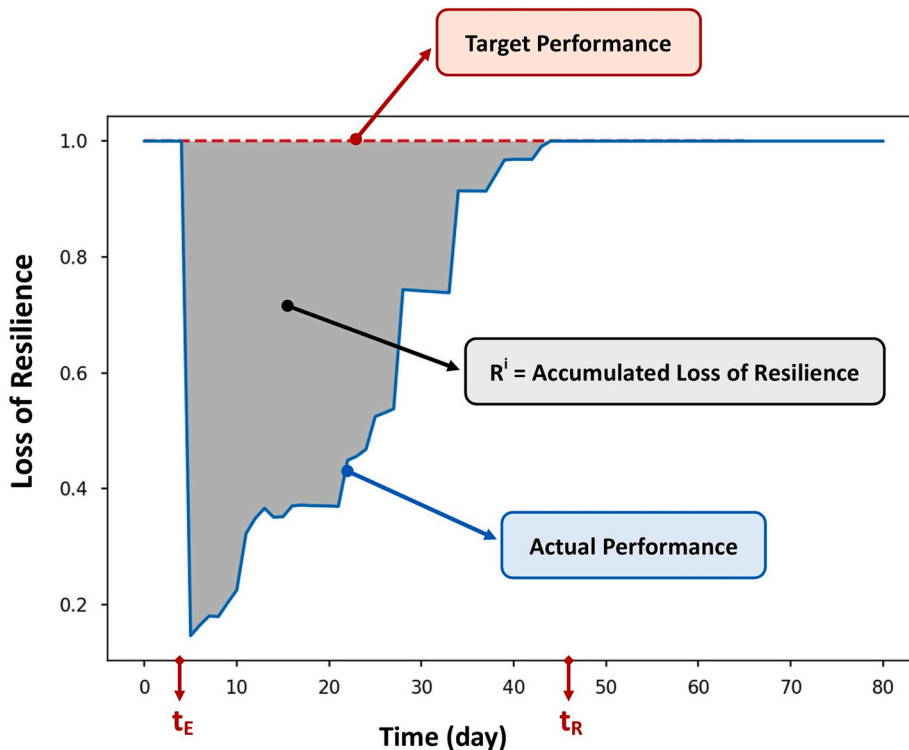

Fig. 4. Illustration of the CIS Accumulated Resilience Metric (ALR) R^i (Eq. (2)) used in this study.

resilience metric is then:

$$R^i = \int_{t_E}^{t_R} \left(\frac{C_{sys}^{pre,i}(t)}{D_{sys}^{pre,i}(t)} - \frac{C_{sys}^{post,i}(t)}{D_{sys}^{post,i}(t)} \right) dt \tag{2}$$

In this study, pre-disruption performance is assumed to have no Loss of Resilience, thus $P_{pre}^i = 1$, and the target post-disruption performance is assumed to be equal to the pre-disruption performance. Fig. 4 graphically demonstrates that the resilience metric R^i is equal to the area between the target and the actual performance curves of the infrastructure system, computed by integrating the consumption/demand ratio difference in each time step. Thus, the resilience metric R^i for a CIS is the called the Accumulated Loss of Resilience (ALR).

Due to connections, dependencies, and interactions between different infrastructure networks in a community, interdependent CISs are modeled as a "system-of-systems" [63]. As explained in the next section, a resilient behavior of interdependent system of CISs relies on the functioning of all individual infrastructure networks in the community. Conversely, non-resilient behavior of the system of CISs may be induced by interdependencies and cascading failures, where non-performance of one CIS disables otherwise undamaged components of other CISs. To capture this system-of-CIS behavior in a single resilience metric, according to [66], a linear combination (i.e., weighted sum) of the performance of each infrastructure system, measured using the joint Accumulated Loss of Resilience (SoCIS-ALR) metric, is proposed as:

$$R^{SoCIS} = \sum_{i \in CIS} \omega_i R^i = \sum_{i \in CIS} \omega_i \cdot \int_{t_E}^{t_R} \left(\frac{C_{sys}^{pre,i}(t)}{D_{sys}^{pre,i}(t)} - \frac{C_{sys}^{post,i}(t)}{D_{sys}^{post,i}(t)} \right) dt \tag{3}$$

$$s.t. \sum_{i \in CIS} \omega_i = 1 \tag{4}$$

where ω_i denotes the predetermined weights assigned to individual CISs, for example, according to the relative importance of each network in the community. In this paper, the relative importance of infrastructure networks in the community is considered equal for power, natural gas, and water networks. Since the SoCIS-ALR metric R^{SoCIS} is normalized and unitless, it can evaluate the performance of interdependent CISs joinly regardless of the type of service provided by the infrastructure system. Moreover, using R^{SoCIS} facilitates computing the community resilience performance goals proposed in NIST SP-1190 [64].

2.4. Simulation module

The function of this module is to simulate the post-disruption performance of the interdependent CIS system-of-systems during the recovery process. To capture the interdependency, this module models the interactions between different infrastructure networks during the post-disaster recovery process by tracking the initial damage and function recovery of CIS components. The following sections describe the simulation module.

2.4.1. Modeling of interdependent CISs

Different types of interdependencies exist between the infrastructure systems, such as physical, cyber, geographical, and logical [6]. According to the relevant studies on resilience quantification, a multi-layer network model can be used to represent interdependent CISs [8,62,65]. In this model, different CISs can operate and interact through the interdependency links connecting nodes from different CISs. An illustrative example of a multi-layer network with interdependency links is provided in Fig. 5. As depicted in this figure, the service inputs necessary for continuing the functionality of an infrastructure network are transferred from other infrastructure networks through such
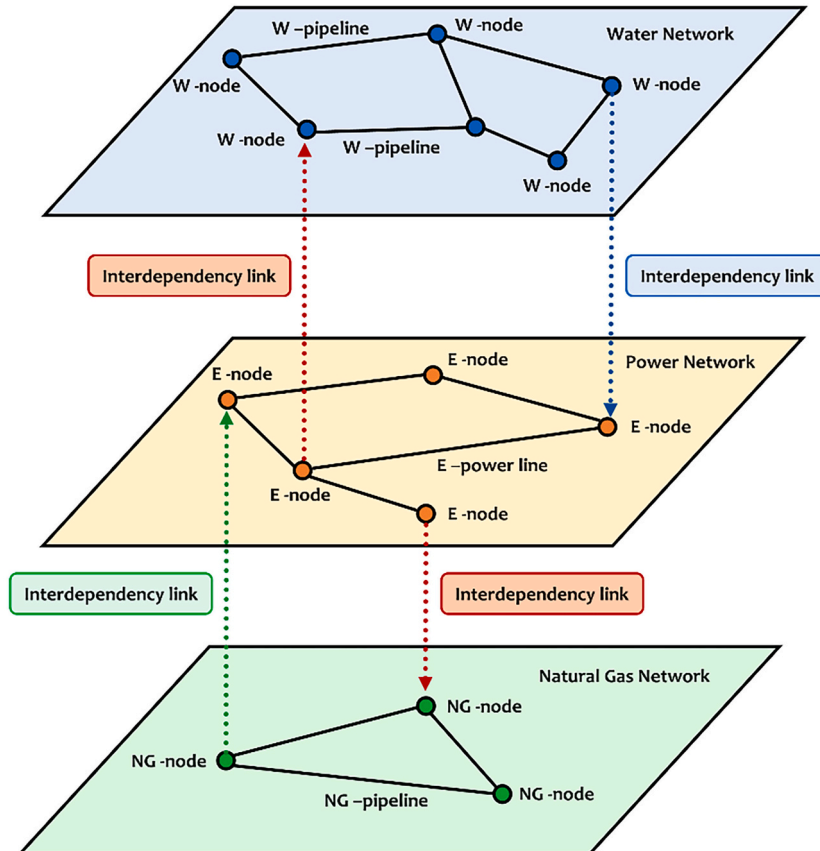

Fig. 5. An illustrative example of a multilayer network with interdependency links.

interdependency links. These interdependency links represent the physical interdependencies between various infrastructure networks. The principal interdependencies between power, natural gas, and water networks are physical [27,62]. In addition to physical, the simulation module in the Res-IOS framework considers the geographical interdependencies between the infrastructure networks. Geographical interdependencies between CISs occur when their components are located in proximity to one another so that those components may be simultaneously affected by the same natural hazard [8]. The cyber and the logical interdependencies are not modeled in this study.

2.4.2. Network flow-based model of an infrastructure system

There are different CIS operation models for analyzing the performance of infrastructure systems and its evaluation through the post-disaster recovery process [66–69]. Considering the characteristics of the CISs addressed in this paper, power, natural gas, and water, a network flow-based operation model is selected to capture the evolution of infrastructure systems' performance according to [8,25,70–72]. In this operation model, the function of each infrastructure system is to generate and convey a specific type of service throughout its network.

To represent an infrastructure system as a network, it is crucial to map the physical facilities in the infrastructure system to the set of nodes and links describing the actual functional role of those facilities. The network flow-based model has three types of nodes to differentiate the physical facilities in the infrastructure system by their function type: supply, demand, and transmission. The supply nodes are the facilities in the infrastructure network that generate a service. The demand nodes are the locations in the infrastructure network where the services are delivered to the end users. The transmission nodes are the facilities in the infrastructure network that facilitate service transfer between supply and demand nodes. Another flow-based network component is the links, which connect two nodes to transfer services.

2.4.3. Modeling the recovery process

The recovery process in the simulation module is modeled for three types of interdependent infrastructure systems: electrical power, water, and natural gas. Since the risk assessment module estimates the impact of the disaster on the components of both the demand and supply sides, not only the restoration of infrastructure networks' components but also the demand evolution of consumers is considered in the modeling of the recovery process. In addition to considering time-dependent demands for resources and services during the recovery process, the recovery model of the ResQ-IOS framework can deal with temporary demands for services in the course of the restoration of the damaged components.

According to the components' damage level data, which is stored in the first layer of the ResQ-IOS database, the simulation modules appraise the functionality level of the infrastructure networks. The operational state of the components is evaluated by fuzzy membership functions. Therefore, the operating state of a component after a disaster can be rated as fully functional, partially functional, or completely failed. The amount of time needed to restore a damaged component is a function of its immediate post-disaster damage state, thus a function of the intensity of the hazard at the location of a component and its vulnerability.

The recovery model developed for the ResQ-IOS framework can apply different recovery functions to the damaged CIS components. Besides binary and linear recovery functions, the recovery model implements nonlinear recovery functions. A nonlinear recovery model considers different repair rates throughout the recovery process, made possible and used by the optimization solver in the Iterative Optimization-based Simulation framework.

Due to budget constraints and the limited number of crew teams and resources, it is only feasible for a few failed components to be restored simultaneously. Hence, the availability of resources and maintenance crew teams influences the component repair start time. There are different strategies for sequencing the repairs of the damaged components. The ResQ-IOS framework recovery model can adopt various

restoration sequence strategies for repairing the damaged components in the network. In this paper, the ResQ-IOS framework utilizes a criticality-based strategy applying performance-based (i.e., supply capacity and demand-based) importance approach to specify the restoration sequence of damaged components located at nodes in the interdependent CISs (i.e., nodes with the largest demand are repaired first), and a capacity-based method to determine the sequence of links (e.g., pipelines) to be repaired (i.e., links with the largest capacity are repaired first).

2.5. Optimization module

An optimization solver is embedded into the ResQ-IOS framework to determine the optimal flow of resources and services from and to each node in the considered infrastructure networks to minimize the loss of resilience of interdependent CISs at each step of the recovery process. Thus, the optimization solver is called in each iteration of the ResQ-IOS framework. The optimization module calls for information about the current infrastructure network status stored in the second layer of the ResQ-IOS database. Then, the optimization module updates the mathematical model of the interdependent CISs according to the networks' status parameters. The main parts of the mathematical model, including the objective function and the constraints, stay unchanged; however, the model parameters and some decision variable coefficients may change in an optimization cycle.

2.5.1. Mathematical formulation of the optimization model

In the optimization module, the performance of interdependent infrastructure systems is formulated as a Mixed-Integer Linear Programming (MILP) problem. The resilience of these interdependent infrastructure systems is then quantified by solving the optimization problem. To construct the optimization model for resilience assessment, it is necessary to develop the constraints according to the network flow-based model of infrastructure systems. The constraints of the MILP problem for the power, natural gas, and water CISs used for the optimization module of this paper are presented in Appendix A. The IBM CPLEX solver [73] is utilized to solve the MILP problem.

In this study, the resilience of an infrastructure system is quantified using the resilience metric defined by Eq. (3). Measuring the best performance that considered interdependent CISs in each step of the recovery process is essential. An infrastructure system with optimal service distribution throughout its network may cope with the aftermaths of a natural disaster better than an infrastructure system with random service dispatching. The optimal service dispatch within a network usually reduces the unmet demand and results in a higher resilience value for that network. The objective of the optimization module is to minimize the SoCIS-ALR metric, which measures the loss of resilience for interdependent critical infrastructure systems after a disruption, and it is expressible as follows:

$$\min_{DV} R_t^{SoCIS} = \min_{DV} \sum_{i \in CIS} \omega_i R_t^i = \min_{DV} \sum_{i \in CIS} \omega_i \cdot \left(\frac{C_{sys}^{pre,i}(t)}{D_{sys}^{pre,i}(t)} - \frac{C_{sys}^{post,i}(t)}{D_{sys}^{post,i}(t)} \right) \quad (5)$$

where R_t^{SoCIS} is the instantaneous accumulated loss of resilience for interdependent infrastructure systems and ω_i and R_t^i denote the predetermined weights assigned to individual CISs and the instantaneous accumulated loss of resilience for an individual CIS, respectively. In the objective function (Eq. (5)), R_t^i, the accumulated loss of resilience for an individual CIS, is the difference between the instantaneous target (i.e., pre-disruption) and the instantaneous actual (i.e., post-disruption) performance of the concerned CIS. The instantaneous performance of the concerned CIS is the ratio of the instantaneous total consumption of its service $C_{sys}^i(t)$ and the instantaneous total demand for its service $D_{sys}^i(t)$. $\left(\frac{C_{sys}^{pre,i}(t)}{D_{sys}^{pre,i}(t)} \right)$ and $\left(\frac{C_{sys}^{post,i}(t)}{D_{sys}^{post,i}(t)} \right)$ denote the ratios for the pre-disruption and post-

disruption performance of the concerned CIS i at time step t.

Then, to minimize the loss of resilience at each time step of the resilience assessment period, the optimal post-disruption performance of the interdependent infrastructure systems is calculated by considering the constraints related to the network topology, the operating state of facilities, and interdependency between the infrastructure systems (Eqs. (A.1)-(A.86)). The optimization model for the SoCIS-ALR metric for the three considered interdependent CISs (power, natural gas, and water) is formulated as follows:

$$
\begin{aligned}
\min_{DV} R_t^{SoCIS} &= \min_{DV} \sum_{i \in CIS} \omega_i \cdot \left(\frac{C_{sys}^{pre,i}(t)}{D_{sys}^{pre,i}(t)} - \frac{C_{sys}^{post,i}(t)}{D_{sys}^{post,i}(t)} \right) \\
&= \min_{DV} \sum_{i \in CIS} \omega_i \cdot \left(\frac{\sum_{s \in SN^i} \sum_{f \in SF^i} C_{f,s,t}^{pre,i}}{\sum_{s \in SN^i} \sum_{f \in SF^i} D_{f,s,t}^{pre,i}} - \frac{\sum_{s \in SN^i} \sum_{f \in SF^i} C_{f,s,t}^{post,i}}{\sum_{s \in SN^i} \sum_{f \in SF^i} D_{f,s,t}^{post,i}} \right) \\
&= \min_{DV} \left[\omega_E \cdot \left(\frac{\sum_{m \in NEf_e} \sum_{e \in FE} E_{C,t}^{f_e,m,pre}}{\sum_{m \in NEf_e} \sum_{e \in FE} D_{E,t}^{f_e,m,pre}} - \frac{\sum_{m \in NEf_e} \sum_{e \in FE} E_{C,t}^{f_e,m,post}}{\sum_{m \in NEf_e} \sum_{e \in FE} D_{E,t}^{f_e,m,post}} \right) \right. \\
&\quad + \omega_G \cdot \left(\frac{\sum_{n \in NGf_g} \sum_{g \in FG} G_{C,t}^{f_g,n,pre}}{\sum_{n \in NGf_g} \sum_{g \in FG} D_{G,t}^{f_g,n,pre}} - \frac{\sum_{n \in NGf_g} \sum_{g \in FG} G_{C,t}^{f_g,n,post}}{\sum_{n \in NGf_g} \sum_{g \in FG} D_{G,t}^{f_g,n,post}} \right) \\
&\quad \left. + \omega_W \cdot \left(\frac{\sum_{j \in NWf_w} \sum_{w \in FW} W_{C,t}^{f_w,j,pre}}{\sum_{j \in NWf_w} \sum_{w \in FW} D_{W,t}^{f_w,j,pre}} - \frac{\sum_{j \in NWf_w} \sum_{w \in FW} W_{C,t}^{f_w,j,post}}{\sum_{j \in NWf_w} \sum_{w \in FW} D_{W,t}^{f_w,j,post}} \right) \right]
\end{aligned}
\tag{6}
$$

$$s.t. \quad \text{sets of constraints } [Eqs.(A.1) - (A.86)]$$

where R_t^{SoCIS} denotes the instantaneous joint accumulated loss of resilience for interdependent CISs. ω_i is assigned weights to each infrastructure system. ω_E, ω_G, and ω_W represent the predetermined weights of the power, natural gas, and water networks. As explained earlier for Eq. (5), $C_{sys}^i(t)$ and $D_{sys}^i(t)$ are the instantaneous total consumption and demand for the service provided by the concerned CIS i. The variable $C_{f,s,t}^{post,i}$ denotes that the instantaneous total consumption of the service in the CIS i after the disruption equals the total service consumption by facilities f belonging to the CIS i (SF^i) and located at the node s in the network of the CIS i (SN^i). The variable $D_{f,s,t}^{post,i}$ denotes that the instantaneous total demand for the service provided by the CIS i equals the total post-disruption demands for the service requested by facilities f belonging to the CIS i (SF^i) and located at the node s in the network of the CIS i (SN^i). The same definitions apply to pre-disruption situations. Symbols $E_{C,t}$, $G_{C,t}$, and $W_{C,t}$ denote the instantaneous consumption of electric power, natural gas, and water, respectively. $D_{E,t}$, $D_{G,t}$, and $D_{W,t}$ are the instantaneous demand for electric power, natural gas, and water, respectively. The information about other indices and variables in Eq. (6) is given in the nomenclature of this paper.

3. Case study

Shelby County, located in Tennessee (TN), USA, is selected to demonstrate the capabilities of the ResQ-IOS framework proposed in this paper. The power, natural gas, and water networks of Shelby County can be considered realistic examples for the resilience assessment of interdependent infrastructure networks. The data on Shelby County's power, natural gas, and water networks, including the topology, demand, supply capacity, and interdependencies between the infrastructure networks, is obtained from [74,75]. However, the authors reasonably assumed some missing data, particularly for the natural gas network. For better understanding, the nodal demands are normalized to the total demand of the respective infrastructure network. This normalization applies to the nodal supply capacities as well.

The authors employ a slightly modified version of Shelby County's infrastructure networks to demonstrate the capabilities of the ResQ-IOS framework for quantifying the resilience of interdependent CISs. For instance, there is no power plant in Shelby County. To resolve such a problem, a node in the power network containing a PGS is replaced with a CCPP such that the power generation capacity of the CCPP is equal to the amount of electrical power imported into Shelby County by the PGS. This assumption is made to avoid changing the actual flow pattern in the network. Subsequently, this modification creates more interdependency relations between the gas, power, and water networks. The interdependency relations between infrastructure networks in Shelby County are illustrated in Fig. 6. This figure demonstrates how different sectors of the power, gas, and water networks are interconnected. Two bidirectional interdependency relations exist: one between the power generation and natural gas production sectors and another between the power generation and water supply sectors. Also, this figure shows that the operability of the water and natural gas transmission sectors relies on the proper functioning of the power transmission grid. For instance, the production capacity of the natural gas network can be affected
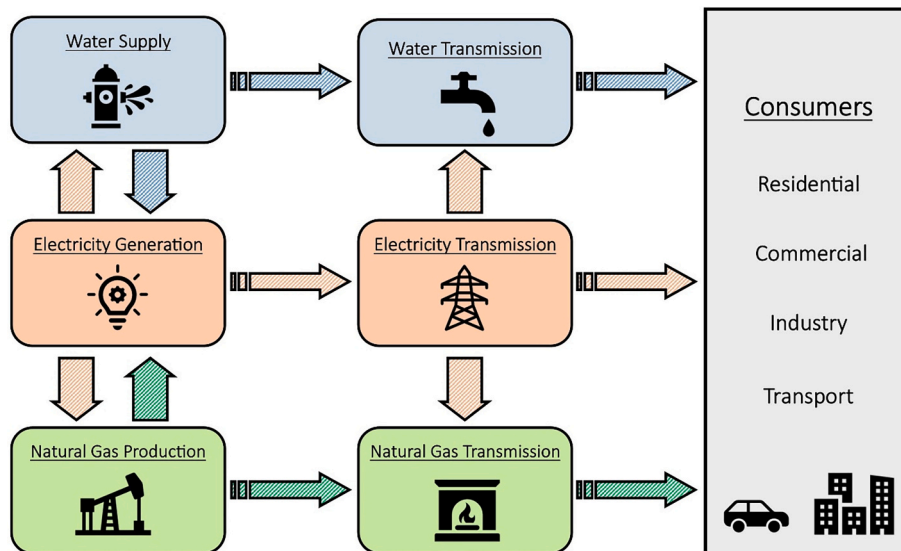

Fig. 6. The interdependency relations between infrastructure networks in the case study.
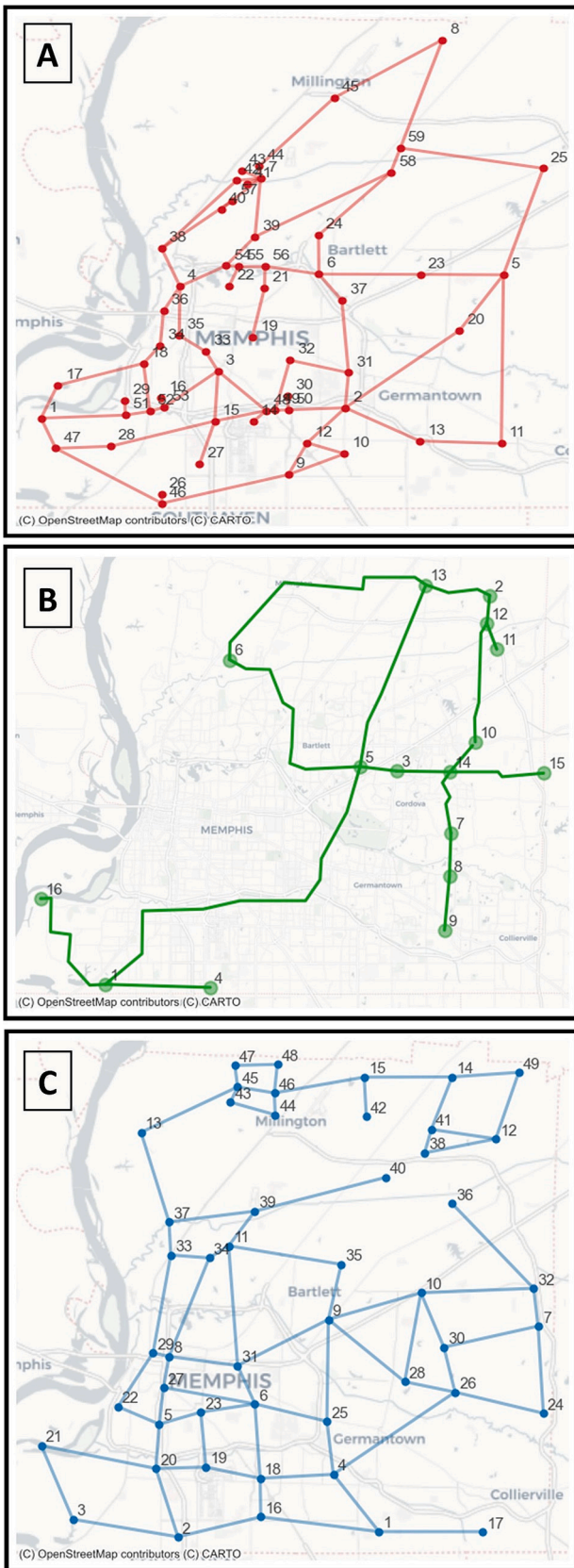
Fig. 7. Topologies of the (A) power, (B) natural gas, (C) water infrastructure networks in Shelby County (TN), USA (Map tiles by CARTO, under CC-BY 4.0).

adversely by natural hazards like an earthquake. This reduction in natural gas supply capacity can curtail the electricity generation capacity and, subsequently, influence the power supply to the transmission and supply components of the water network. Thus, a disruption in the natural gas network can reduce water service delivery to consumers, whereas there is no direct interdependency relation between the natural gas and water networks, according to Fig. 6.

Fig. 7 displays the topologies of Shelby County's infrastructure networks at the transmission level. The power, natural gas, and water networks are depicted in red, green, and blue colors, respectively. The modified power network comprises 73 powerlines and 59 electric nodes: one CCPP, two GTPPs, 5 PGSs, seventeen 23-kV ESSs, twenty 12-kV ESSs, and 14 power intersections. The modified natural gas network contains 17 pipelines and 16 gas nodes: one LNGT, one NGPP, two NGCSs, one NGGS, and 11 regular distribution stations. The modified water infrastructure network consists of 49 water nodes and 71 pipelines. There are 6 WSTs, 4 WPSs, and 5 WSFs. The remaining nodes are water intersections that deliver water to the end users. In this study, it is assumed that all nodes and links within Shelby County's infrastructure networks are subject to the destructive impacts of the considered natural hazard.

4. Results and discussion

To demonstrate the capabilities of the ResQ-IOS framework to model the interdependency between the infrastructure systems and evaluate the resilience of those interdependent systems against disasters, the seismic resilience of the interdependent CISs located in Shelby County (TN), USA is quantified. The data relating to damage functions, functionality levels, and the details of the recovery process for the CISs' components (e.g., the required time for restoring a component) is obtained from the HAZUS Earthquake Model Technical Manual (HAZUS 5.1) published by Federal Emergency Management Agency (FEMA) in July 2022 [53]. To show the performance evolution of infrastructure networks (power, natural gas, and water) after a disaster, a hazard scenario is defined similarly to the realistic earthquake scenario in Shelby County provided by [76]. The hazard scenario simulates an earthquake with a magnitude of Mw = 7.7 and an epicenter located at 35.3 N and 90.3 W (situated in the northwest of Shelby County). The performance evolution of the Shelby County infrastructure networks after this earthquake scenario is shown in Fig. 8. This figure displays the changes in the actual performance of power, natural gas, and water networks considering the hazard occurs on day 0, and the recovery process starts on day 1. To calculate the resilience metric defined by Eq. (2). (i.e., accumulated loss of resilience), the area between the target and the actual performance of each network is computed according to Fig. 4. The Accumulated Loss of Resilience (ALR) metrics for the power, natural gas, and water CISs are 9.47, 12.32, and 15.37 days, respectively. For a better understanding of ALR, we can interpret the ALR of an infrastructure network as the equivalent number of days that the infrastructure network of interest is completely shut down (i.e., the met demand is zero). For instance, the ALR of the power network is 9.47 days, meaning total unmet demand during the recovery process that takes 54 days to complete equals 9.47 days with zero power supply. The minimum instantaneous performance of the power system $P^i(t)$ (the consumption/demand LR) was 17.3% of the daily demand in this earthquake scenario.

It is noteworthy that the ALR determines the amount of unmet demand during the recovery process of an infrastructure network after the disaster. Still, this ALR resilience metric does not specify the speed of the recovery process. In other words, an infrastructure network with a lower ALR value may have a more extended recovery period; for example, the case study (Fig. 8) reveals that the ALR for the natural gas network (12.32) is higher than power network (9.47), while the function recovery of the natural gas network is completed in 18 days, 36 days
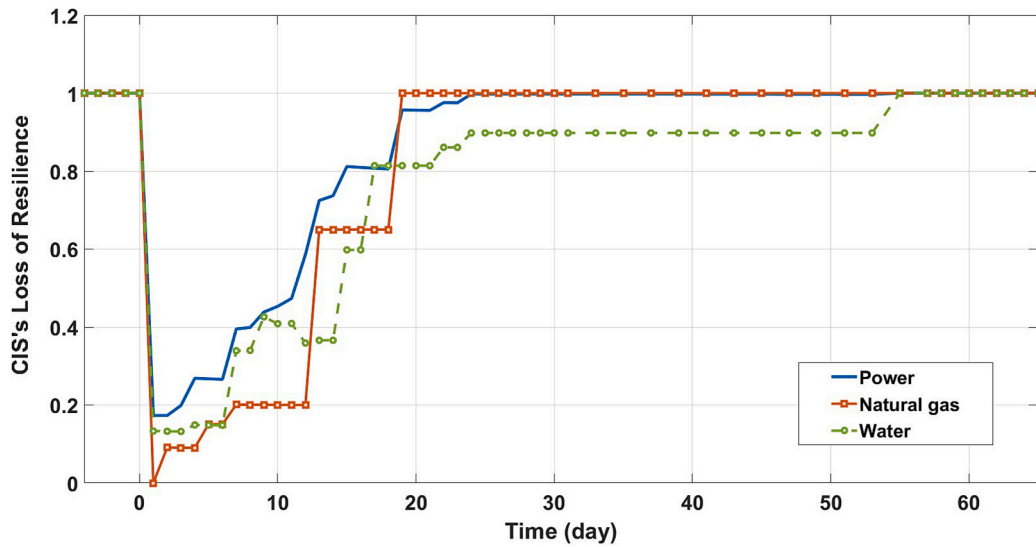
Fig. 8. The performance evolution of the Shelby County CISs in the investigated earthquake scenario (The earthquake occurs on day 0, and the recovery process starts on day 1).
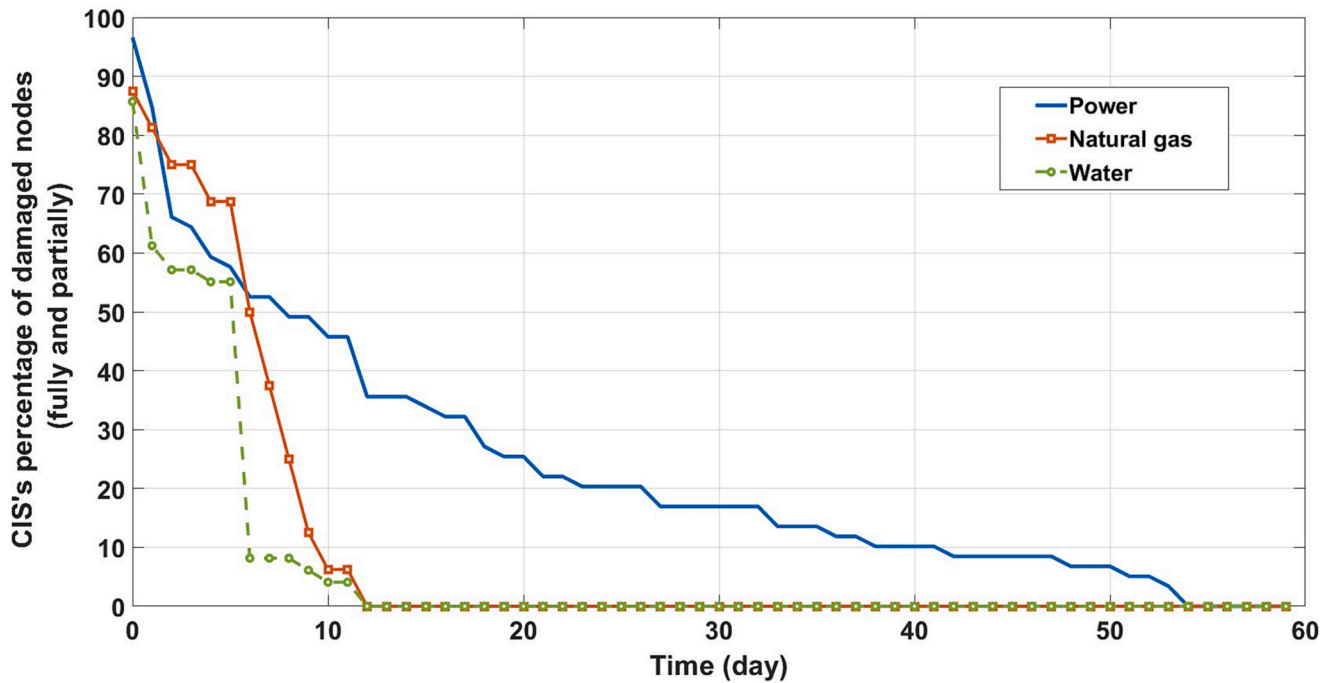

Fig. 9. The daily percentage of partially and fully damaged nodes in the Shelby County CISs during the recovery process after the investigated earthquake scenario ($M_w = 7.7$).

sooner than the power network's recovery period (54 days). Although the natural gas network holds the fastest rate in the recovery process, this network is the only infrastructure network in the case study that totally failed for a short period (one day), as shown in Fig. 8.

According to the results of resilience quantification, the water network has the highest ALR among the three Shelby County CISs; however, the water network is not the last infrastructure system recovered from earthquake-induced failures. Fig. 9 indicates the daily percentage of partially and fully damaged nodes in the CISs' networks in Shelby County during the recovery process after the earthquake. According to Fig. 9, the restoration of the water network's components has been completed in 12 days, almost 4.5 times faster than that of the power network. Despite the relatively fast restoration of the damaged

components in the water network, the resilience indicator for the water network cannot approach value of one earlier than the 54th day of the recovery process. The main reason for such post-disaster recovery of the

Table 1
The required time to restore the different percentages of the Shelby County interdependent CISs' services.

Required time (days)		Percentage of service recovery			
		30%	60%	90%	100%
Network	Power	7	13	19	54
	Natural gas	13	13	18	18
	Water	7	16	54	54

water network is the interdependency between the power and water networks. Due to the slower recovery rate of the power network, the operability of some components in the water network, such as water pump stations, is conditioned on the functionality level of the power network's elements, like substations and power lines. Namely, the constant part of the water network's resilience curve between the 23rd day and 52nd day of the recovery process in Fig. 8 (the recovery process starts on day 1) is due to the water pump station located at node 11 being out of service during the period mentioned above even though its earthquake-induced damage is fully restored and the water pipelines connected to the pump station are ready to operate. The reason for the inoperability of this water pump station is the lack of power supply delivered by the connected 12-kV electric substation due to ongoing components' restoration in the power network.

It is important to note that the damage recovery of the natural gas network (i.e., the restoration of direct earthquake-induced damage to the natural gas network) is completed in 12 days, according to Fig. 9, whereas the function recovery of the natural gas network is completed in 18 days according to Fig. 8. The main reason for this 6-day delay in the function recovery of the gas network is the interdependency between the power and natural gas networks. In other words, the natural gas network cannot reach full production capacity after the 12th day because of insufficient power supply by the electricity grid. Fig. 9 also provides some information concerning the robustness of the individual CISs in the case study. According to this figure, the power network has the lowest robustness to the earthquake scenario since 96.6% of its nodes are partially or fully damaged on the first day after the occurrence of the earthquake. In contrast, the water network is the most robust infrastructure network in Shelby County after the earthquake. In Fig. 9, the slope of the curve indicates the instantaneous (daily) rate of damage recovery (i.e., the restoration of direct earthquake-induced damage) for the concerned infrastructure network in Shelby County. The ResQ-IOS framework enables the evaluation of the functional recovery metrics proposed in the NIST SP-1190 report [64] to quantify the function restoration time aspect of the recovery process. Table 1 shows the required time to restore the different percentages of interdependent CISs' services in the case study.

To evaluate the resilience of an urban community against natural hazards, it is essential to jointly quantify the resilience of the community's interdependent CISs. The SoCIS-ALR metric for the system-of-CISs in this Shelby Count case study is calculated using Eq. (3). Fig. 10 depicts the evolution of the joint accumulated loss of resilience (SoCIS-ALR metric) for three earthquake scenarios with magnitudes 6.8, 7.7, and 8.2 and the same epicenter. The computed SoCIS-ALR values for the three earthquakes are 4.40, 12.36, and 18.53, while the recovery period for the community, starting from day 1, lasts 20, 54, and 62 days, respectively, as shown in Fig. 10. This figure demonstrates the capability of the ResQ-IOS to consider all components of interdependent CISs for community resilience assessment that reflects one of the contributions of this study.

The seismic resilience of the interdependent CISs in the ResR-IOS framework is quantified by considering constraints on the resources for the recovery process, such as limits on the number of Repair and Maintenance (R&M) teams for each type of component within the infrastructure networks. For this purpose, the ResQ-IOS framework can import the number of available R&M teams for 13 types of components belonging to three interdependent CISs in the Shelby County case study, and then simulate restoring the failed components based on the restoration sequence that is determined according to the limits on the number of R&M teams and the strategy adopted for the recovery process of the Shelby County infrastructure networks. To illustrate the effect of the number of available R&M teams on the recovery process, the seismic resilience of the interdependent CISs for two cases is assessed. In addition to the case with the initial number of R&M teams, a modified case evaluates the resilience of Shelby County CISs considering a 50% increase in the number of the power network's R&M teams and a simultaneous 50% decrease in the number of the water network's R&M teams.

Fig. 11 displays the evolution of joint accumulated loss of resilience (SoCIS-ALR metric) to compare the initial and rebalanced R&M team assignment. The results of this figure point out that rebalancing the assignment of R&M teams improves the SoCIS-ALR measure by 30.8%. Also, the rebalancing of R&M team assignments leads to the recovery of the Shelby County CISs in 36 days, 18 days sooner than with the initial R&M team assignment. As discussed earlier, the reason for this resilience improvement is that the power network is the controlling infrastructure in the recovery of the Shelby County CISs after the case study earthquake. It means the power-dependent infrastructure systems like the water network and, accordingly, the community cannot return to their normal conditions before the power network's recovery process is completed.

To investigate the effect of R&M team configuration on the post-earthquake resilience of the Shelby County interdependent CISs, the R&M teams for repairing the water pipelines are reconfigured. The default configuration of the water pipeline R&M teams is four persons
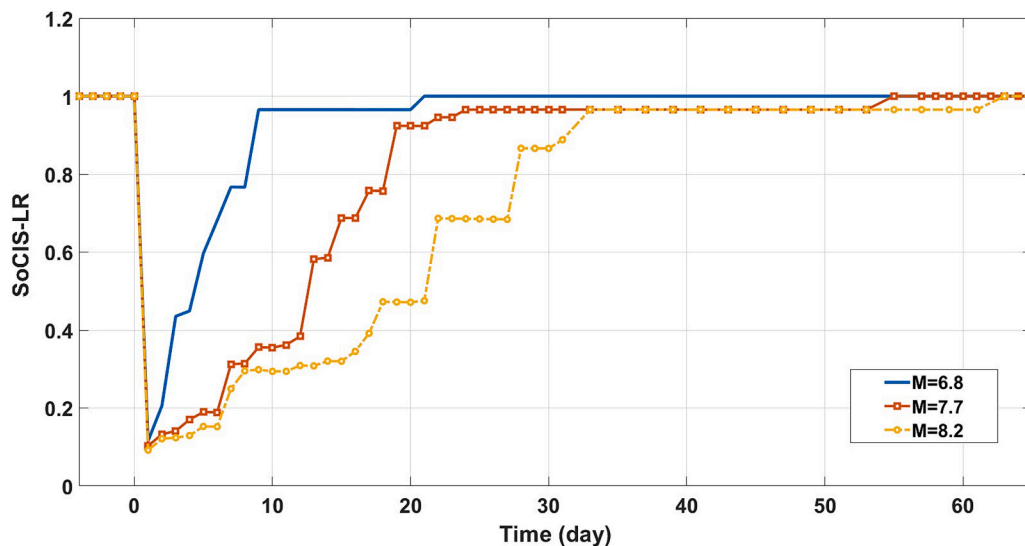

Fig. 10. The SoCIS-ALR joint resilience assessment of the Shelby County CISs for three earthquake scenarios (The earthquake occurs on day 0, and the recovery process starts on day 1).
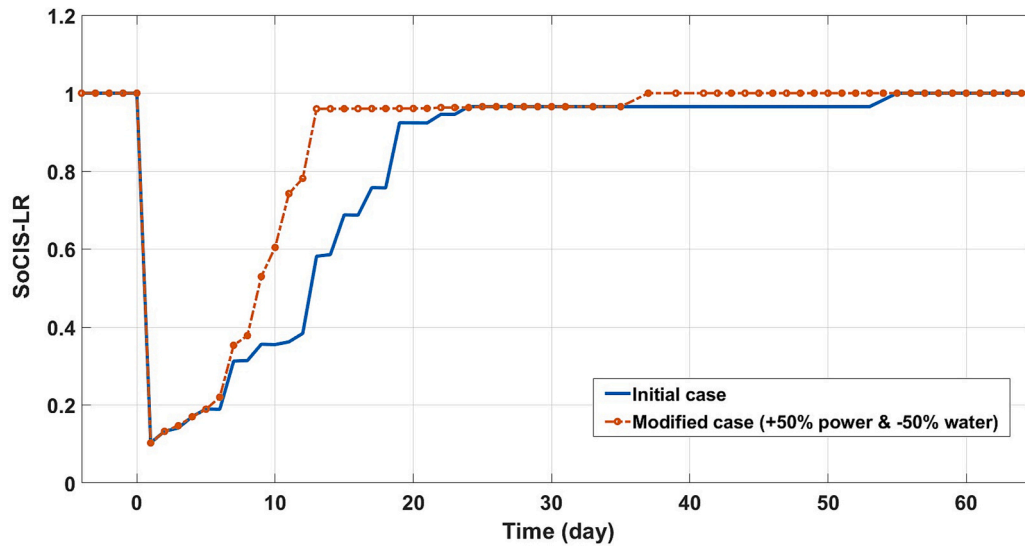
Fig. 11. The joint resilience assessment of the Shelby County interdependent CISs comparing the initial and the re-balanced R&M team assignment (The earthquake occurs on day 0, and the recovery process starts on day 1).
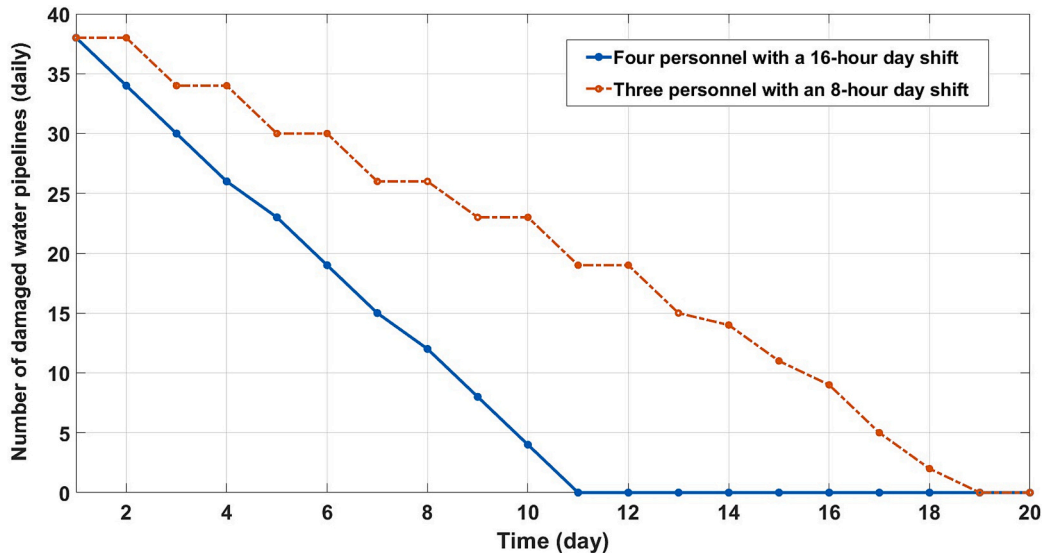

Fig. 12. The daily number of damaged water pipelines during the recovery of the Shelby County water network after the earthquake with a magnitude of 8.5 for two configurations of R&M teams.

Table 2
The fully functional recovery duration and SoCIS-ALR metric values for the Shelby County interdependent CISs after the earthquake with $M_w = 7.7$ with varying supply margins.

Scenario	SoCIS-ALR	% Changes wrt. The initial case	Recovery duration	% Changes wrt. The initial case
Initial case	12.36	–	54	–
+10% in the supply capacity of the power network	12.22	1.133%	54	0%
+10% in the supply capacity of the natural gas network	12.20	1.295%	54	0%
+10% in the supply capacity of the water network	10.92	11.65%	24	55.5%

with a 16-h workday. The water pipeline R&M teams' configuration is changed to three people with an 8-h workday, while keeping the number for water pipeline R&M teams the same. Fig. 12 illustrates that different R&M team configurations change the required time for repairing the damaged water pipelines. In the default case, all damaged pipelines are repaired at an almost constant repair rate after 11 days. However, repairing the damaged pipelines with smaller R&M teams who work shorter shifts takes 19 days, as shown in Fig. 12. Also, this figure indicates another contribution of this paper: the required time for restoring the damaged components can take several time steps in the resilience assessment period. Although the recovery process of damaged water pipelines is affected by changing the R&M teams' configuration, the effect on the Shelby County SoCIS-ALR is negligible. As discussed earlier, due to the interdependency between water and power infrastructure systems, the full recovery of the water network is conditioned on the rate of the power network's recovery process.

One strategy to enhance the Shelby County interdependent CIS resilience is to improve the robustness of the individual CIS by providing

extra supply capacity margins. Three scenarios are devised to determine whether adding extra supply capacity to the infrastructure networks significantly impacts the seismic resilience of the Shelby County system-of-CISs. Those three scenarios consider a 10% increment in the supply capacity of each of the power, natural gas, and water networks, respectively, while keeping the supply capacity of the other two networks unchanged. The results of the resilience analyses for these scenarios are given in Table 2.

While the 10% increase in the supply capacity of the power grid and natural gas network improves the Shelby County SoCIS-ALR metric slightly, a 10% percent increment in the water network's supply capacity significantly shortens the time to fully recover the function of all three Shelby County CISs. It is important to note that after the community returns to normal conditions on the 24th day of the recovery process, restoring the failed components in the power network will continue until the 54th day. Also, the water pump station at node 11 is still out of service after the 24th day due to the lack of power supply. Nevertheless, the water network provides water to meet the nodal demands previously supplied by the water pump station located at node 11 because of the increased capacity of other water supply facilities that can compensate for the inoperability of the pump station at node 11. The network distributes the water flow by optimally mapping new routes from the supply nodes to the demand nodes, dependent on the pump station at node 11. This optimal distribution of water service results from the contribution of this study that the ResQ-IOS is capable of determining the optimal flow of resources and services throughout infrastructure networks.

Concerning the performance of the power network, since the power supply of the pump station at node 11 is no longer a top priority demand, the ResQ-IOS optimization module re-dispatches the power supply to other nodes with higher priority. On the 24th day, the power network can supply the total demand, except for the pump station at node 11. This reflects other contributions of this paper that the ResQ-IOS can consider the components' time-dependent demands and temporary loads that may be imposed on infrastructure networks during the recovery process. Hence, all infrastructure networks in the case study can meet the daily demands after the day 24th, which means the Shelby County CIS function is fully restored after the case study earthquake scenario. On the 54th day, the power network's recovery is completed, and the aforementioned water pump station can start supplying water to the connected nodes. Notably, after the 54th day, the water network utilizes about 91% of its supply capacity.

In order to gain an insight into the relation between the seismic hazard and the seismic resilience of the Shelby County interdependent CISs, case study resilience analyses were done for earthquakes with the magnitude varying between $M_w = 6$ and $M_w = 9$ and the same epicenter. In addition to SoCIS-ALR, the required time for a full recovery of all Shelby County CISs is calculated. Fig. 13 demonstrates the relation between the magnitude of the seismic hazard and the seismic resilience of the interdependent CISs in Shelby County. As shown in Fig. 13, the SoCIS-ALR metric values increase monotonically from 0.279 for the $M_w = 6$ earthquake to 23.22 for the $M_w = 9$ earthquake, an increase of 83-fold, but not at the same rate. Furthermore, the SoCIS-ALR metric saturates at earthquake $M_w = 8.5$. The time to fully recover the joint function of the Shelby County interdependent CISs varies from six to 62 days. Notably, the full functional recovery time saturates at $M_w = 8.0$. The cause of such saturation is that the power network that controls the community's recovery duration reaches the maximum level of function degradation during the $M_w = 8.0$ earthquake scenario, with the number of damaged nodes (including both total and partial damage) is 57 and 58 (out of 59 nodes) after the $M_w = 8.0$ and $M_w = 8.2$ earthquakes, respectively. The SoCIS-ALR metric is still sensitive to the number of damaged power CIS nodes, saturating after the $M_w = 8.5$ earthquake.

5. Conclusions

Critical Infrastructure Systems (CISs), providing services and essential resources to modern societies, are currently highly complex, interconnected, and interdependent. On the one hand, growing interdependency and complexity between infrastructure networks and, on the other hand, frequent exposure to extreme events such as natural hazards have increased the probability of cascading failures and, consequently, the prolonged lack of serviceability in urban communities. Hence, the resilience analysis of interdependent CISs to natural hazards is quickly coming into the stakeholders' focus. To this end, this paper presents the ResQ-IOS framework, an efficient Iterative Optimization-based Simulation (IOS) framework to model interdependent critical infrastructure systems, simulate their post-disaster performance considering interdependencies, and quantify their individual and joint resilience using integral and instantaneous resilience metrics. The ResQ-IOS framework takes advantage of both simulation-based and optimization-based approaches to evaluate the natural hazard resilience of the interdependent CISs and thus addresses existing research gaps.

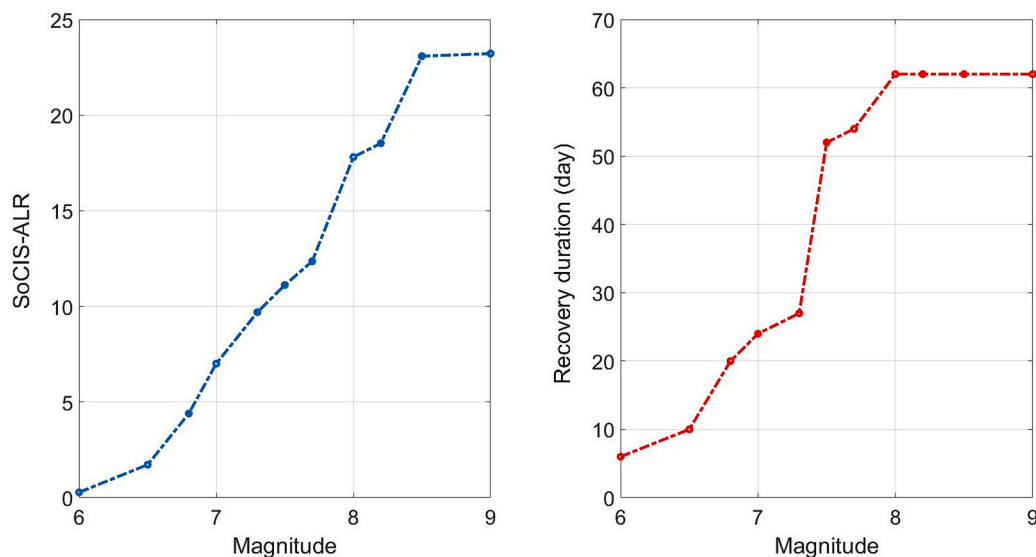The ResQ-IOS framework comprises five modules, namely, the risk

Fig. 13. The time to full (100%) function recovery and the SoCIS-ALR metric values for the Shelby County interdependent CISs as a function of the case study earthquake magnitude.

assessment, simulation, optimization, database, and controller modules. The risk assessment module simulates the hazard and evaluates the vulnerability of the infrastructure networks' components. The data concerning the post-disaster status of the infrastructure networks is populated in the database module. Then, the simulation module utilizes this data to simulate the performance evolution of infrastructure networks. The simulated data is conveyed to the database and is later used by the optimization module to maximize the post-disruption performance of interdependent CISs by determining the optimal flow of services and resources in these infrastructure networks. The simulation module reconfigures the supply and demand patterns to optimize infrastructure systems' performance in one step of the recovery process. It then simulates the evolution of infrastructure networks' performance in the next step of the recovery process. This time-stepping procedure is repeated between the simulation, database, and optimization modules. Meanwhile, the controller module calculates the loss of resilience for interdependent CISs at each time step and ends the time-stepping process once the prescribed stopping criteria are satisfied.

The resilience analysis presented in the case study demonstrates the capabilities of the ResQ-IOS framework to consider real-world conditions of the infrastructure systems' components after a disaster and the functioning of these systems in impaired states during the recovery process. The ResQ-IOS framework evaluates the post-disaster functionality level of the infrastructure networks' components by using a fuzzy logic-based model. This framework considers a varying required time for restoring the damaged components as a function of the damage state of the component and the configuration of the respective repair and maintenance teams. Moreover, the damaged component repair start time depends on the number and configuration of the available repair and maintenance teams and the restoration sequence of the components according to the selected component recovery prioritization strategy defined at the CIS level. The ResQ-IOS framework is capable of following various strategies for specifying the restoration sequence of damaged components. Importantly, in addition to these factors confined to a CIS, the operability of a component highly relies on its demands being supplied by its own CIS as well as by the other CIS in the system-of-CISs that support a community. The interdependencies among the CIS are modeled in this way. The ResQ-IOS framework is able to consider the time-dependent evolution of demands for resources and services during the resilience assessment period of interdependent CISs. During the recovery process, the ResQ-IOS framework can also take into account temporary loads (i.e., demands) that may be imposed on infrastructure networks due to the ongoing restoration process of the damaged components.

The seismic resilience quantification of the Shelby County case study indicates the recovery of an urban community relies on the performance evolution of the interdependent CISs providing the essential resources and services to the community. The results of the case study seismic resilience assessment demonstrate that the recovery duration of the community may be controlled by the performance evolution of one infrastructure system among the interdependent CISs. For this case study, the controlling infrastructure is the power CIS, as the community cannot return to pre-disaster status before the recovery of the power network is accomplished. The community's recovery duration varies with several factors, such as the number of repair and maintenance teams and their configuration, as well as the CIS recovery strategy selected for specifying the restoration sequence of the damaged components. As for applying resilience enhancement measures in the case study, the resilience assessment results point out that increasing the supply capacity of individual CIS is most effective for the water network, shortening the time to full functional recovery duration by 55% and improving the system-of-CIS resilience metric SoCIS-ALR by about 12%. This finding is not obvious, since the Shelby County case study power CIS controls the recovery process. Another resilience enhancing measure, focused on rebalancing and reconfiguring the repair and

maintenance teams, is however quite effective in terms of speeding up the recovery of the power CIS, and the overall Shelby County system of interdependent CISs.

The ResQ-IOS has been developed to act as a powerful and versatile computational tool for quantifying and analyzing the resilience of interdependent CISs. This computational tool can be used to plan resilience-oriented sustainable development of urban communities by, for example, specifying Renewable Energy (RE)-based strategies. The ResQ-IOS framework, with its focus on energy systems, can identify the beneficial effects of RE-based strategies. For instance, ResQ-IOS established that a water pump station's inoperability might benefit from deploying a local RE-based power system as a backup to remarkably shorten the time to full recovery of the case study system-of-CISs. Considering backup systems for important nodes in infrastructure networks, such as equipping water supply facilities with emergency on-site power systems, may enhance the resilience of interdependent CISs for a period during the recovery process. An interesting topic for future studies is to investigate the durability of such backup systems to supply the required demands in case of the prolonged recovery of the community.

Enhancing the resilience of interdependent CISs to natural hazards by specifying the optimal recovery strategy and pre- and post-disaster resilience-enhancing measures, such as decreasing component vulnerability or increasing the amount of recovery resources, while introducing RE-based systems and backup systems into the networks is the topic for future research enabled by the ResQ-IOS framework presented in this framework. Hence, the authors suggest conducting a comprehensive study on the inter-coupling of energy sectors, including the utilization of renewable energy systems and energy storage technologies. Integrating economic models into the ResQ-IOS framework could further enable stakeholders to investigate and adopt the most cost-effective recovery strategies, considering simultaneously pre- and post-disaster resilience-enhancing measures and renewable energy sources, to improve the disaster resilience of their communities.

CRediT authorship contribution statement

Declaration of Competing Interest

The authors declare that they have no known competing financial interests or personal relationships that could have appeared to influence the work reported in this paper.

Data availability

No data was used for the research described in the article.

Acknowledgments

Appendix A

A.1. Power network operating constraints

In the network flow-based model of the power system, the supply nodes are the electrical power generation sites and the gate stations for electricity import. This paper considers two types of power plants: Gas Turbine Power Plants (GTPPs) and Combined-Cycle Power Plants (CCPPs). A Power Gate Station (PGS) used for electricity import is considered a supply node in this paper. The transmission nodes are the electric substations. The demand nodes are the locations where the power is delivered to the end users, such as building stock units, water pump stations, etc. The links represent power transmission lines installed between various parts of the power network.

The constraints of the power network are represented by Eqs. (A.1)-(A.6). Eq. (A.1) guarantees the flow conservation at each power network node. Eq. (A.2) states that the power flow injected to each node at each time step comprises the electricity imported by the PGSs and the electrical power output of GTPP and CCPP units. Eq. (A.3) describes that the power flow out of each node at each time step is equal to the accumulated electrical power consumed by the GTPP, CCPP, and ESS units in the power network, NGPP, LNG terminals, and NGCS units from the natural gas network, WSF, and WPS units in the water network and building stock units including different types of buildings. Eq. (A.4) ensures that the power flow through each power transmission line at each time step cannot exceed the power line's capacity if the power line is operational. The logical relationships between the operating state of the power line and the operating state of its start and terminal nodes are represented by Eqs. (A.5)-(A.6).

$$\sum_{(p \in LE \mid T(p)=m)} e_t^p - \sum_{(p \in LE \mid S(p)=m)} e_t^p + E_{G,t}^m - E_{C,t}^m = 0 \quad \forall m \in NE, \forall t \in T \tag{A.1}$$

$$E_{G,t}^m = E_{G,t}^{GTPP,m} + E_{G,t}^{CCPP,m} + E_{G,t}^{PGS,m} \quad \forall m \in NE, \forall t \in T \tag{A.2}$$

$$E_{C,t}^m = E_{C,t}^{GTPP,m} + E_{C,t}^{CCPP,m} + E_{C,t}^{ESS,m} + E_{C,t}^{NGPP,m} + E_{C,t}^{LNGT,m} + E_{C,t}^{NGCS,m} + E_{C,t}^{WSF,m} + E_{C,t}^{WPS,m} + \sum_{(H \in BSU \mid loc(H)=m)} E_{C,t}^H \quad \forall m \in NE, \forall t \in T \tag{A.3}$$

$$0 \leq e_t^p \leq z_{E,t}^p \cdot e_{cap}^p \quad \forall p \in LE, \forall t \in T \tag{A.4}$$

$$z_{E,t}^p \leq x_{E,t}^{S(p)} \quad \forall p \in LE, \forall t \in T \tag{A.5}$$

$$z_{E,t}^p \leq x_{E,t}^{T(p)} \quad \forall p \in LE, \forall t \in T \tag{A.6}$$

A.2. Natural gas network operating constraints

Regarding the natural gas system's network flow-based model, the supply nodes represent the facilities where natural gas is prepared for sending out into the transmission grid, such as LNG terminals, Natural Gas Processing Plants (NGPP), and Natural Gas Gate Stations (NGGS) employed for natural gas imports. Transmission nodes are representative of the natural gas compressor stations. The demand nodes provide natural gas to consumers, such as power plants, building stock units, etc. The links are the natural gas pipelines connecting the gas network nodes.

Eqs. (A.7)-(A.12) represent the constraints of the natural gas network. The conservation of flow at each node of the natural gas network is represented by Eq. (A.7). Eq. (A.8) states that the inflow of natural gas at each node at each time step includes the natural gas imported by NGGS and the natural gas processed by the NGPP unit and LNG terminal. Eq. (A.9) describes that the natural gas outflow at each node at each time step is the accumulated natural gas consumed by the GTPP and CCPP units in the power network, NGPP unit, LNG terminal, and NGCS units in the natural gas network, and building stock units. Eq. (A.10) ensures that the natural gas flow through each pipeline at each time step does not exceed the pipeline's capacity, provided that the pipeline is operational. Eqs. (A.11)-(A.12) describes the logical relationships between the operating state of the pipeline and the nodes connected to the pipeline.

$$\sum_{(q \in LG \mid T(q)=n)} g_t^q - \sum_{(q \in LG \mid S(q)=n)} g_t^q + G_{G,t}^n - G_{C,t}^n = 0 \quad \forall n \in NG, \forall t \in T \tag{A.7}$$

$$G_{G,t}^n = G_{G,t}^{LNGT,n} + G_{G,t}^{NGPP,n} + G_{G,t}^{NGGS,n} \quad \forall n \in NG, \forall t \in T \tag{A.8}$$

$$G_{C,t}^n = G_{C,t}^{GTPP,n} + G_{C,t}^{CCPP,n} + G_{C,t}^{NGPP,n} + G_{C,t}^{LNGT,n} + G_{C,t}^{NGCS,n} + \sum_{(H \in BSU \mid loc(H)=n)} G_{C,t}^H \quad \forall n \in NG, \forall t \in T \tag{A.9}$$

$$0 \leq g_t^q \leq z_{G,t}^q \cdot g_{cap}^q \quad \forall q \in LG, \forall t \in T \tag{A.10}$$

$$z_{G,t}^q \leq x_{G,t}^{S(q)} \quad \forall q \in LG, \forall t \in T \tag{A.11}$$

$$z_{G,t}^q \leq x_{G,t}^{T(q)} \quad \forall q \in LG, \forall t \in T \tag{A.12}$$

A.3. Water network operating constraints

The supply and transmission nodes represent the water supply facilities, water storage tanks, and pump stations in the water system's network flow-based model. Demand nodes are where water is provided to the consumers, like building stock units. Links are representative of the water

pipelines located between different parts of the water network.

Eqs. (A.13)-(A.22) constitute the constraints of the water network. Eq. (A.13) displays the water flow balance equation at each water network node at each time step. Eq. (A.14) declares that the inflow of water at each node at each time step equals the amount of water supplied by the WSF and WST units. Eq. (A.15) states that the water flow out of each node at each time step consists of the water consumed by the CCPP and building stock units. Eq. (A.16) demonstrates that if the pipeline is operational, the water flow at each time step does not exceed the pipeline's capacity. A water pipeline's operating state relies on the nodes' operating state at the end of that pipeline, as shown in Eqs. (A.17)-(A.18).

$$\sum_{(l \in LW \mid T(l)=j)} w_t^l - \sum_{(l \in LW \mid S(l)=j)} w_t^l + W_{G,t}^j - W_{C,t}^j = 0 \quad \forall j \in NW, \forall t \in T \tag{A.13}$$

$$W_{G,t}^j = W_{G,t}^{WSF,j} + W_{G,t}^{WST,j} \quad \forall j \in NW, \forall t \in T \tag{A.14}$$

$$W_{C,t}^j = W_{C,t}^{CCPP,j} + \sum_{(H \in BSU \mid loc(H)=j)} W_{C,t}^H \quad \forall j \in NW, \forall t \in T \tag{A.15}$$

$$0 \leq w_t^l \leq z_{W,t}^l \cdot w_{cap}^l \quad \forall l \in LW, \forall t \in T \tag{A.16}$$

$$z_{W,t}^l \leq x_{W,t}^{S(l)} \quad \forall l \in LW, \forall t \in T \tag{A.17}$$

$$z_{W,t}^l \leq x_{W,t}^{T(l)} \quad \forall l \in LW, \forall t \in T \tag{A.18}$$

A.4. Modeling the interdependencies between the infrastructure systems

In this research, interdependency between two infrastructure systems refers to two aspects of the relationship between the infrastructure systems. The first aspect is the reliance of an infrastructure system's performance on the service delivery of another infrastructure system. Taking a water pump station as an example, the functionality of the pump station is dependent on the electric power supplied by the power network. This aspect is modeled by interdependency links coupling two nodes from two infrastructure networks interacting with one another. This interdependency link transfers the service from a node in the supplier infrastructure network to another node in the consumer infrastructure network. In the case of a pump station, the electric power needed for the pump station's functionality is transferred by the interdependency link from the supplier node in the power network to the consumer node in the water network. The supplier node, which delivers service to consumer nodes in other infrastructure networks, often acts as a demand node in its network [62,70]. The operating state of the interdependency link is considered a binary (0–1) variable [71,77]. If the supplier node meets the required demand of the consumer node in another network, then the interdependency link will be operational. Otherwise, the service transfer between supplier and consumer nodes through the interdependency link will cease. The inoperability of the interdependency link may lead to the loss of operation in the consumer node's network.

The second aspect of interdependency considered in this paper is that the recovery process of an infrastructure system may adversely affect the restoration of the facilities in another infrastructure network. For instance, the structural damages to the pump station may be fully restored after an earthquake, but the station is still not functional due to the lack of power supply. Hence, the power network's recovery process can delay the restoration of the pump station. The constraints described in the following section represent both aspects of the considered interdependency.

A.5. Interdependency constraints

This section presents the interdependency constraints of facilities belonging to three types of infrastructure networks: power, natural gas, and water. As for the power network, the interdependency constraints of GTPP, CCPP, PGS, ESS, and BSU are provided. Interdependency constraints are developed for LNGT, NGPP, NGGS, NGCS, and BSU in the natural gas network. Regarding the water network, WSF, WPS, WST, and BSU are considered for interdependency constraints. Eqs. (A.19)-(A.21) represent the time delay in starting the recovery process at each node, including the response time needed for the decision-making on the recovery of damaged nodes. For instance, if a node in the power network faces a 5-day delay in providing the prerequisites of the recovery process because of the road closure, this delay may postpone the beginning of the restoration of facilities located at the respective node.

Eqs. (A.22)-(A.28) state that the performance of a GTPP depends on the availability of the coupled gas node with the electric node where the facility is located, as well as the operation state of the interdependency link between those nodes. Eqs. (A.29)-(A.39) declare that the operation of a CCPP is dependent on the availability of the coupled gas and water nodes with the electric node where the CCPP is located and the functionality of two interdependency links originating from the connected gas and water nodes. Eqs. (A.40) and (A.41) represent the constraints concerning the restoration of a PGS. Eqs. (A.42)-(A.44) represent the interdependency constraints regarding the restoration of an ESS. Eq. (A.45) describes that electric power consumed by BSUs located in the service area of an electric node will not exceed their time-dependent demand if the respective electric node is operational.

$$x_{E,t}^m \leq \tau_{E,t}^m \quad \forall m \in NE, \forall t \in T \tag{A.19}$$

$$x_{G,t}^n \leq \tau_{G,t}^n \quad \forall n \in NG, \forall t \in T \tag{A.20}$$

$$x_{W,t}^j \leq \tau_{W,t}^j \quad \forall j \in NW, \forall t \in T \tag{A.21}$$

$$0 \leq E_{G,t}^{GTPP,m} \leq \varphi_{E,t}^{GTPP,m} \cdot S_{E,t}^{GTPP,m} \quad \forall m \in NE, \forall t \in T \tag{A.22}$$

$$0 \leq E_{C,t}^{GTPP,m} \leq \varphi_{E,t}^{GTPP,m} \cdot D_{E,t}^{GTPP,m} \quad \forall m \in NE, \forall t \in T \tag{A.23}$$

$$0 \leq G_{C,t}^{GTPP,n} \leq \delta_t^{GTPP,n}.D_{G,t}^{GTPP,n} \quad \forall n \in NG, \forall t \in T \tag{A.24}$$

$$\varphi_{E,t}^{GTPP,m} \leq x_{E,t}^m \quad \forall m \in NE, \forall t \in T \tag{A.25}$$

$$\delta_t^{GTPP,n} \leq x_{G,t}^n \quad \forall n \in NG, \forall t \in T \tag{A.26}$$

$$G_{C,t}^{GTPP,n} - \theta_t^{GTPP,n}.D_{G,t}^{GTPP,n} \geq 0 \quad \forall n \in NG, \forall t \in T \tag{A.27}$$

$$\varphi_{E,t}^{GTPP,m} \leq \theta_t^{GTPP,n} \quad \forall (n,m) \in IGtE, \forall t \in T \tag{A.28}$$

$$0 \leq E_{G,t}^{CCPP,m} \leq \varphi_{E,t}^{CCPP,m}.S_{E,t}^{CCPP,m} \quad \forall m \in NE, \forall t \in T \tag{A.29}$$

$$0 \leq E_{C,t}^{CCPP,m} \leq \varphi_{E,t}^{CCPP,m}.D_{E,t}^{CCPP,m} \quad \forall m \in NE, \forall t \in T \tag{A.30}$$

$$0 \leq G_{C,t}^{CCPP,n} \leq \delta_t^{CCPP,n}.D_{G,t}^{CCPP,n} \quad \forall n \in NG, \forall t \in T \tag{A.31}$$

$$\varphi_{E,t}^{CCPP,m} \leq x_{E,t}^m \quad \forall m \in NE, \forall t \in T \tag{A.32}$$

$$\delta_t^{CCPP,n} \leq x_{G,t}^n \quad \forall n \in NG, \forall t \in T \tag{A.33}$$

$$G_{C,t}^{CCPP,n} - \theta_t^{CCPP,n}.D_{G,t}^{CCPP,n} \geq 0 \quad \forall n \in NG, \forall t \in T \tag{A.34}$$

$$\varphi_{E,t}^{CCPP,m} \leq \theta_t^{CCPP,n} \quad \forall (n,m) \in IGtE, \forall t \in T \tag{A.35}$$

$$0 \leq W_{C,t}^{CCPP,j} \leq \gamma_t^{CCPP,j}.D_{W,t}^{CCPP,j} \quad \forall j \in NW, \forall t \in T \tag{A.36}$$

$$\gamma_t^{CCPP,j} \leq x_{W,t}^j \quad \forall j \in NW, \forall t \in T \tag{A.37}$$

$$W_{C,t}^{CCPP,j} - \sigma_t^{CCPP,j}.D_{W,t}^{CCPP,j} \geq 0 \quad \forall j \in NW, \forall t \in T \tag{A.38}$$

$$\varphi_{E,t}^{CCPP,m} \leq \sigma_t^{CCPP,j} \quad \forall (j,m) \in IWtE, \forall t \in T \tag{A.39}$$

$$0 \leq E_{G,t}^{PGS,m} \leq \varphi_{E,t}^{PGS,m}.S_{E,t}^{PGS,m} \quad \forall m \in NE, \forall t \in T \tag{A.40}$$

$$\varphi_{E,t}^{PGS,m} \leq x_{E,t}^m \quad \forall m \in NE, \forall t \in T \tag{A.41}$$

$$0 \leq E_{C,t}^{ESS,m} \leq \varphi_{E,t}^{ESS,m}.D_{E,t}^{ESS,m} \quad \forall m \in NE, \forall t \in T \tag{A.42}$$

$$\varphi_{E,t}^{ESS,m} \leq x_{E,t}^m \quad \forall m \in NE, \forall t \in T \tag{A.43}$$

$$E_{C,t}^{ESS,m} - x_{E,t}^m.D_{E,t}^{ESS,m} \geq 0 \quad \forall m \in NE, \forall t \in T \tag{A.44}$$

$$0 \leq \sum_{(H \in BSU | loc(H)=m)} E_{C,t}^H \leq x_{E,t}^m . \sum_{(H \in BSU | loc(H)=m)} D_{E,t}^H \quad \forall m \in NE, \forall t \in T \tag{A.45}$$

Eqs. (A.46)-(A.52) describe that the operating state of a LNGT relies on the availability of the coupled electric node with the gas node where the LNGT is located and the functionality of the interdependency link between those gas and electric nodes. Eqs. (A.53)-(A.59) mean that a NGPP's performance is dependent on the availability of the coupled electric node with the gas node where the NGPP is located and the operation state of the interdependency link between those nodes. Eqs. (A.60) and (A.61) represent the constraints regarding the restoration of a NGGS. The interdependency constraints related to the NGCS are constituted by Eqs. (A.62)-(A.68). Eq. (A.69) ensures that the amount of natural gas consumed by BSUs located in the service area of a gas node cannot exceed their demand if the respective gas node is operational.

$$0 \leq G_{G,t}^{LNGT,n} \leq \varphi_{G,t}^{LNGT,n}.S_{G,t}^{LNGT,n} \quad \forall n \in NG, \forall t \in T \tag{A.46}$$

$$0 \leq G_{C,t}^{LNGT,n} \leq \varphi_{G,t}^{LNGT,n}.D_{G,t}^{LNGT,n} \quad \forall n \in NG, \forall t \in T \tag{A.47}$$

$$0 \leq E_{C,t}^{LNGT,m} \leq \pi_t^{LNGT,m}.D_{E,t}^{LNGT,m} \quad \forall m \in NE, \forall t \in T \tag{A.48}$$

$$\varphi_{G,t}^{LNGT,n} \leq x_{G,t}^n \quad \forall n \in NG, \forall t \in T \tag{A.49}$$

$$\pi_t^{LNGT,m} \leq x_{E,t}^m \quad \forall m \in NE, \forall t \in T \tag{A.50}$$

$$E_{C,t}^{LNGT,m} - \alpha_t^{LNGT,m}.D_{E,t}^{LNGT,m} \geq 0 \quad \forall m \in NE, \forall t \in T \tag{A.51}$$

$$\varphi_{G,t}^{LNGT,n} \leq \alpha_t^{LNGT,m} \quad \forall (m,n) \in IEtG, \forall t \in T \tag{A.52}$$

$$0 \leq G_{G,t}^{NGPP,n} \leq \varphi_{G,t}^{NGPP,n}.S_{G,t}^{NGPP,n} \quad \forall n \in NG, \forall t \in T \tag{A.53}$$

$$0 \leq G_{C,t}^{NGPP,n} \leq \varphi_{G,t}^{NGPP,n}.D_{G,t}^{NGPP,n} \quad \forall n \in NG, \forall t \in T \tag{A.54}$$

$$0 \leq E_{C,t}^{NGPP,m} \leq \pi_t^{NGPP,m}.D_{E,t}^{NGPP,m} \quad \forall m \in NE, \forall t \in T \tag{A.55}$$

$$\varphi_{G,t}^{NGPP,n} \leq x_{G,t}^n \quad \forall n \in NG, \forall t \in T \tag{A.56}$$

$$\pi_t^{NGPP,m} \leq x_{E,t}^m \quad \forall m \in NE, \forall t \in T \tag{A.57}$$

$$E_{C,t}^{NGPP,m} - \alpha_t^{NGPP,m}.D_{E,t}^{NGPP,m} \geq 0 \quad \forall m \in NE, \forall t \in T \tag{A.58}$$

$$\varphi_{G,t}^{NGPP,n} \leq \alpha_t^{NGPP,m} \quad \forall (m,n) \in IEtG, \forall t \in T \tag{A.59}$$

$$0 \leq G_{G,t}^{NGGS,n} \leq \varphi_{G,t}^{NGGS,n}.S_{G,t}^{NGGS,n} \quad \forall n \in NG, \forall t \in T \tag{A.60}$$

$$\varphi_{G,t}^{NGGS,n} \leq x_{G,t}^n \quad \forall n \in NG, \forall t \in T \tag{A.61}$$

$$0 \leq G_{C,t}^{NGCS,n} \leq \varphi_{G,t}^{NGCS,n}.D_{G,t}^{NGCS,n} \quad \forall n \in NG, \forall t \in T \tag{A.62}$$

$$\varphi_{G,t}^{NGCS,n} \leq x_{G,t}^n \quad \forall n \in NG, \forall t \in T \tag{A.63}$$

$$G_{C,t}^{NGCS,n} - x_{G,t}^n.D_{G,t}^{NGCS,n} \geq 0 \quad \forall n \in NG, \forall t \in T \tag{A.64}$$

$$0 \leq E_{C,t}^{NGCS,m} \leq \pi_t^{NGCS,m}.D_{E,t}^{NGCS,m} \quad \forall m \in NE, \forall t \in T \tag{A.65}$$

$$\pi_t^{NGCS,m} \leq x_{E,t}^m \quad \forall m \in NE, \forall t \in T \tag{A.66}$$

$$E_{C,t}^{NGCS,m} - \alpha_t^{NGCS,m}.D_{E,t}^{NGCS,m} \geq 0 \quad \forall m \in NE, \forall t \in T \tag{A.67}$$

$$\varphi_{G,t}^{NGCS,n} \leq \alpha_t^{NGCS,m} \quad \forall (m,n) \in IEtG, \forall t \in T \tag{A.68}$$

$$0 \leq \sum_{(H \in BSU|loc(H)=n)} G_{C,t}^H \leq x_{G,t}^n.\sum_{(H \in BSU|loc(H)=n)} D_{G,t}^H \quad \forall n \in NG, \forall t \in T \tag{A.69}$$

Eqs. (A.70)-(A.75) represent that the restoration of a WSF depends on the availability of the coupled electric node with the water node where the facility is located and the operating state of the interdependency link between those water and electric nodes. Eqs. (A.76)-(A.80) display that the recovery of a WPS relies on the availability of the coupled electric node with the water node where the WPS is located and the operation state of the interdependency link between those nodes. Eqs. (A.81) and (A.82) represent the constraints concerning the restoration of a WST. Eq. (A.83) reveals that if a water node is operational, the amount of water consumed by BSUs in that water node's service area cannot exceed their demand.

$$0 \leq W_{G,t}^{WSF,j} \leq \varphi_{W,t}^{WSF,j}.S_{W,t}^{WSF,j} \quad \forall j \in NW, \forall t \in T \tag{A.70}$$

$$0 \leq E_{C,t}^{WSF,m} \leq \pi_t^{WSF,m}.D_{E,t}^{WSF,m} \quad \forall m \in NE, \forall t \in T \tag{A.71}$$

$$\varphi_{W,t}^{WSF,j} \leq x_{W,t}^j \quad \forall j \in NW, \forall t \in T \tag{A.72}$$

$$\pi_t^{WSF,m} \leq x_{E,t}^m \quad \forall m \in NE, \forall t \in T \tag{A.73}$$

$$E_{C,t}^{WSF,m} - \beta_t^{WSF,m}.D_{E,t}^{WSF,m} \geq 0 \quad \forall m \in NE, \forall t \in T \tag{A.74}$$

$$\varphi_{W,t}^{WSF,j} \leq \beta_t^{WSF,m} \quad \forall (m,j) \in IEtW, \forall t \in T \tag{A.75}$$

$$\varphi_{W,t}^{WPS,j} \leq x_{W,t}^j \quad \forall j \in NW, \forall t \in T \tag{A.76}$$

$$0 \leq E_{C,t}^{WPS,m} \leq \pi_t^{WPS,m}.D_{E,t}^{WPS,m} \quad \forall m \in NE, \forall t \in T \tag{A.77}$$

$$\pi_t^{WPS,m} \leq x_{E,t}^m \quad \forall m \in NE, \forall t \in T \tag{A.78}$$

$$E_{C,t}^{WPS,m} - \beta_t^{WPS,m}.D_{E,t}^{WPS,m} \geq 0 \quad \forall m \in NE, \forall t \in T \tag{A.79}$$

$$\varphi_{W,t}^{WPS,j} \leq \beta_t^{WPS,m} \quad \forall (m,j) \in IEtW, \forall t \in T \tag{A.80}$$

$$0 \leq W_{G,t}^{WST,j} \leq \varphi_{W,t}^{WST,j}.S_{W,t}^{WST,j} \quad \forall j \in NW, \forall t \in T \tag{A.81}$$

$$\varphi_{W,t}^{WST,j} \leq x_{W,t}^j \quad \forall j \in NW, \forall t \in T \tag{A.82}$$

$$0 \leq \sum_{(H \in BSU|loc(H)=j)} W_{C,t}^H \leq x_{W,t}^j.\sum_{(H \in BSU|loc(H)=j)} D_{W,t}^H \quad \forall j \in NW, \forall t \in T \tag{A.83}$$

Eqs. (A.84)-(A.86) state that the links in different infrastructure networks (i.e., power lines, pipelines) can convey flow if they are not damaged. In other words, full recovery is a necessary condition for links to be operational in the network.

$$z_{E,t}^p \leq \mu_{E,t}^p \quad \forall p \in LE, \forall t \in T \tag{A.84}$$

$$z_{G,t}^q \leq \mu_{G,t}^q \quad \forall q \in LG, \forall t \in T \tag{A.85}$$

$$z_{W,t}^l \leq \mu_{W,t}^l \quad \forall l \in LW, \forall t \in T \tag{A.86}$$

References

[1] Zhou Y, Li J, Wang G, Chen S, Xing W, Li T. Assessing the short-to medium-term supply risks of clean energy minerals for China. J Clean Prod Apr. 2019;215: 217–25. https://doi.org/10.1016/j.jclepro.2019.01.064.

[2] Mirkhani S, Saboohi Y. Stochastic modeling of the energy supply system with uncertain fuel price - a case of emerging technologies for distributed power generation. Appl Energy 2012;93:668–74. https://doi.org/10.1016/j.apenergy.2011.12.099.

[3] Ahmadi S, Saboohi Y, Vakili A. Frameworks, quantitative indicators, characters, and modeling approaches to analysis of energy system resilience: a review. Renew Sustain Energy Rev Jul. 01, 2021;144. https://doi.org/10.1016/j.rser.2021.110988.

[4] Hafeznia H, Yousefi H, Razi Astaraei F. A novel framework for the potential assessment of utility-scale photovoltaic solar energy, application to eastern Iran. Energ Conver Manage Nov. 2017;151:240–58. https://doi.org/10.1016/j.enconman.2017.08.076.

[5] Gillessen B, Heinrichs H, Hake JF, Allelein HJ. Natural gas as a bridge to sustainability: infrastructure expansion regarding energy security and system transition. Appl Energy Oct. 2019;251. https://doi.org/10.1016/j.apenergy.2019.113377.

[6] Rinaldi SM, Peerenboom JP, Kelly TK. Identifying, understanding, and analyzing critical infrastructure interdependencies. IEEE Control Syst Magaz 2001;21(6): 11–25. https://doi.org/10.1109/37.969131.

[7] Ouyang M. Review on modeling and simulation of interdependent critical infrastructure systems. Reliab Eng Syst Safety 2014;121:43–60. https://doi.org/10.1016/j.ress.2013.06.040.

[8] Kong J, Zhang C, Simonovic SP. Optimizing the resilience of interdependent infrastructures to regional natural hazards with combined improvement measures. Reliab Eng Syst Saf Jun. 2021;210. https://doi.org/10.1016/j.ress.2021.107538.

[9] Jufri FH, Widiputra V, Jung J. State-of-the-art review on power grid resilience to extreme weather events: Definitions, frameworks, quantitative assessment methodologies, and enhancement strategies. Appl Energy Apr. 01, 2019;239: 1049–65. https://doi.org/10.1016/j.apenergy.2019.02.017.

[10] Zeng Z, Fang YP, Zhai Q, Du S. A Markov reward process-based framework for resilience analysis of multistate energy systems under the threat of extreme events. Reliab Eng Syst Saf May 2021;209. https://doi.org/10.1016/j.ress.2021.107443.

[11] Panteli M, Mancarella P. Influence of extreme weather and climate change on the resilience of power systems: impacts and possible mitigation strategies. Electr Pow Syst Res Jun. 29, 2015;127:259–70. https://doi.org/10.1016/j.epsr.2015.06.012. Elsevier Ltd.

[12] Ouyang M, Wang Z. Resilience assessment of interdependent infrastructure systems: with a focus on joint restoration modeling and analysis. Reliab Eng Syst Saf Jul. 2015;141:74–82. https://doi.org/10.1016/j.ress.2015.03.011.

[13] Zakernezhad H, Nazar MS, Shafie-khah M, Catalão JPS. Optimal resilient operation of multi-carrier energy systems in electricity markets considering distributed energy resource aggregators. Appl Energy Oct. 2021;299. https://doi.org/10.1016/j.apenergy.2021.117271.

[14] Barnes A, Nagarajan H, Yamangil E, Bent R, Backhaus S. Resilient design of large-scale distribution feeders with networked microgrids. Electr Pow Syst Res Jun. 2019;171:150–7. https://doi.org/10.1016/j.epsr.2019.02.012.

[15] Younesi A, Shayeghi H, Safari A, Siano P. Assessing the resilience of multi microgrid based widespread power systems against natural disasters using Monte Carlo simulation. Energy Sep. 2020;207. https://doi.org/10.1016/j.energy.2020.118220.

[16] Sayed AR, Wang C, Bi T. Resilient operational strategies for power systems considering the interactions with natural gas systems. Appl Energy May 2019;241: 548–66. https://doi.org/10.1016/j.apenergy.2019.03.053.

[17] Garcia-Dia MJ, DiNapoli JM, Garcia-Ona L, Jakubowski R, O'Flaherty D. Concept analysis: resilience. Arch Psychiatr Nurs Dec. 2013;27(6):264–70. https://doi.org/10.1016/j.apnu.2013.07.003.

[18] Proag V. The concept of vulnerability and resilience. Proc Econ Finance 2014;18: 369–76. https://doi.org/10.1016/s2212-5671(14)00952-6.

[19] Peciłło M. The resilience engineering concept in enterprises with and without occupational safety and health management systems. Saf Sci Feb. 2016;82:190–8. https://doi.org/10.1016/j.ssci.2015.09.017.

[20] Peng C, Yuan M, Gu C, Peng Z, Ming T. A review of the theory and practice of regional resilience. In: Sustainable Cities and Society. 29. Elsevier Ltd; Feb. 01, 2017. p. 86–96. https://doi.org/10.1016/j.scs.2016.12.003.

[21] Yoo M, Kim T, Yoon JT, Kim Y, Kim S, Youn BD. A resilience measure formulation that considers sensor faults. Reliab Eng Syst Saf Jul. 2020;199. https://doi.org/10.1016/j.ress.2019.02.025.

[22] Francis R, Bekera B. A metric and frameworks for resilience analysis of engineered and infrastructure systems. In: Reliability Engineering and System Safety. 121. Elsevier Ltd; 2014. p. 90–103. https://doi.org/10.1016/j.ress.2013.07.004.

[23] Zio E. Challenges in the vulnerability and risk analysis of critical infrastructures. Reliab Eng Syst Saf Aug. 2016;152:137–50. https://doi.org/10.1016/j.ress.2016.02.009.

[24] Pickering B, Choudhary R. Quantifying resilience in energy systems with out-of-sample testing. Appl Energy Mar. 2021;285. https://doi.org/10.1016/j.apenergy.2021.116465.

[25] Sang M, Ding Y, Bao M, Li S, Ye C, Fang Y. Resilience-based restoration strategy optimization for interdependent gas and power networks. Appl Energy Nov. 2021; 302. https://doi.org/10.1016/j.apenergy.2021.117560.

[26] Liu X, Fang YP, Zio E. A hierarchical resilience enhancement framework for interdependent critical infrastructures. Reliab Eng Syst Saf Nov. 2021;215. https://doi.org/10.1016/j.ress.2021.107868.

[27] Almoghathawi Y, Barker K, Albert LA. Resilience-driven restoration model for interdependent infrastructure networks. Reliab Eng Syst Saf May 2019;185:12–23. https://doi.org/10.1016/j.ress.2018.12.006.

[28] Dubaniowski MI, Heinimann HR. A framework for modeling interdependencies among households, businesses, and infrastructure systems; and their response to disruptions. Reliab Eng Syst Saf Nov. 2020;203:107063. https://doi.org/10.1016/J.RESS.2020.107063.

[29] Dubaniowski MI, Heinimann HR. Framework for modeling interdependencies between households, businesses, and infrastructure system, and their response to disruptions—application. Reliab Eng Syst Saf Aug. 2021;212:107590. https://doi.org/10.1016/J.RESS.2021.107590.

[30] Sun L, Stojadinovic B, Sansavini G. Agent-based recovery model for seismic resilience evaluation of electrified communities. Risk Anal Jul. 2019;39(7): 1597–614. https://doi.org/10.1111/RISA.13277.

[31] Sun L, Stojadinovic B, Sansavini G. Resilience evaluation framework for integrated civil infrastructure–community systems under seismic Hazard. J Infrastruct Syst Apr. 2019;25(2):04019016. https://doi.org/10.1061/(ASCE)IS.1943-555X.0000492.

[32] Sun L, D'Ayala D, Fayjaloun R, Gehl P. Agent-based model on resilience-oriented rapid responses of road networks under seismic hazard. Reliab Eng Syst Saf Dec. 2021;216:108030. https://doi.org/10.1016/J.RESS.2021.108030.

[33] Zhao T, Sun L. Seismic resilience assessment of critical infrastructure-community systems considering looped interdependences. Int J Disast Risk Reduct Jun. 2021; 59:102246. https://doi.org/10.1016/J.IJDRR.2021.102246.

[34] Panteli M, Mancarella P. Modeling and evaluating the resilience of critical electrical power infrastructure to extreme weather events. IEEE Syst J Sep. 2017;11 (3):1733–42. https://doi.org/10.1109/JSYST.2015.2389272.

[35] Li G, et al. Risk analysis for distribution systems in the northeast U.S. under wind storms. IEEE Trans Power Syst Mar. 2014;29(2):889–98. https://doi.org/10.1109/TPWRS.2013.2286171.

[36] Rocchetta R, Zio E, Patelli E. A power-flow emulator approach for resilience assessment of repairable power grids subject to weather-induced failures and data deficiency. Appl Energy Jan. 2018;210:339–50. https://doi.org/10.1016/j.apenergy.2017.10.126.

[37] Blagojević N, Kipfer J, Didier M, Stojadinovic B. Probability-based resilience assessment of communities with interdependent civil infrastructure systems. 2020. p. 7d-0020. https://doi.org/10.3929/ETHZ-B-000463549.

[38] Kiran AS. Simulation and Scheduling. In: Handbook of Simulation. John Wiley & Sons, Ltd; 1998. p. 677–717. https://doi.org/10.1002/9780470172445.ch21.

[39] Dehghanimohammadabadi M. Iterative optimization-based simulation (IOS) with predictable and unpredictable trigger events in simulated time. Western New England University; 2016.

[40] April J, Better M, Glover F, Kelly J, Laguna M. Enhancing business process management with simulation optimization. In: Proceedings of the 2006 Winter Simulation Conference; 2006. p. 642–9. https://doi.org/10.1109/WSC.2006.323141.

[41] Dehghanimohammadabadi M, Keyser TK, Cheraghi SH. A novel iterative optimization-based simulation (IOS) framework: an effective tool to optimize system's performance. Comput Ind Eng Sep. 2017;111:1–17. https://doi.org/10.1016/j.cie.2017.06.037.

[42] Syberfeldt A, Karlsson I, Ng A, Svantesson J, Almgren T. A web-based platform for the simulation–optimization of industrial problems. Comput Ind Eng Apr. 2013;64 (4):987–98. https://doi.org/10.1016/J.CIE.2013.01.008.

[43] Göçken M, Dosdoğru AT, Boru A, Geyik F. Characterizing continuous (s, S) policy with supplier selection using simulation optimization. Simulation 2017;93(5): 379–96. https://doi.org/10.1177/0037549716687044.

[44] Klemmt A, Horn S, Weigert G, Wolter KJ. Simulation-based optimization vs. mathematical programming: a hybrid approach for optimizing scheduling problems. Robot Comput Integr Manuf Dec. 2009;25(6):917–25. https://doi.org/10.1016/J.RCIM.2009.04.012.

[45] Chai T, Qin SJ, Wang H. Optimal operational control for complex industrial processes. Annu Rev Control Jan. 2014;38(1):81–92. https://doi.org/10.1016/J.ARCONTROL.2014.03.005.

[46] Figueira G, Almada-Lobo B. Hybrid simulation–optimization methods: a taxonomy and discussion. Simul Model Pract Theory Aug. 2014;46:118–34. https://doi.org/10.1016/J.SIMPAT.2014.03.007.

[47] Lin RC, Sir MY, Pasupathy KS. Multi-objective simulation optimization using data envelopment analysis and genetic algorithm: specific application to determining optimal resource levels in surgical services. Omega (Westport) Oct. 2013;41(5): 881–92. https://doi.org/10.1016/J.OMEGA.2012.11.003.

[48] Lin JT, Chen CM. Simulation optimization approach for hybrid flow shop scheduling problem in semiconductor back-end manufacturing. Simul Model Pract Theory Feb. 2015;51:100–14. https://doi.org/10.1016/J.SIMPAT.2014.10.008.

[49] Wang T, Xu J, Hu JQ, Chen CH. Efficient estimation of a risk measure requiring two-stage simulation optimization. Eur J Oper Res Jun. 2022. https://doi.org/10.1016/J.EJOR.2022.06.028.

[50] Klanke C, Engell S. Scheduling and batching with evolutionary algorithms in simulation-optimization of an industrial formulation plant. Comput Ind Eng Oct. 2022:108760. https://doi.org/10.1016/J.CIE.2022.108760.

[51] Xiao Y, Yoogalingam R. A simulation optimization approach for planning and scheduling in operating rooms for elective and urgent surgeries. Oper Res Health Care Dec. 2022;35:100366. https://doi.org/10.1016/J.ORHC.2022.100366.

[52] Ahmed MA, Alkhamis TM. Simulation optimization for an emergency department healthcare unit in Kuwait. Eur J Oper Res Nov. 2009;198(3):936–42. https://doi.org/10.1016/J.EJOR.2008.10.025.

[53] Federal Emergency Management Agency (FEMA). Hazus earthquake model technical manual, Hazus 5.1. Washington, DC: FEMA; 2022.

[54] Porter Keith A. An overview of PEER's performance-based earthquake engineering methodology. In: Ninth international conference on applications of statistics and probability in civil engineering (ICASP9), San Francisco; Jul. 2003.

[55] Fang Y, Sansavini G. Emergence of antifragility by optimum Postdisruption restoration planning of infrastructure networks. J Infrastruct Syst Dec. 2017;23(4): 04017024. https://doi.org/10.1061/(asce)is.1943-555x.0000380.

[56] Ouyang M, Dueñas-Osorio L. Multi-dimensional hurricane resilience assessment of electric power systems. Struct Safety May 2014;48:15–24. https://doi.org/10.1016/j.strusafe.2014.01.001.

[57] Shen L, Cassottana B, Heinimann HR, Tang LC. Large-scale systems resilience: a survey and unifying framework. Qual Reliab Eng Int Jun. 2020;36(4):1386–401. https://doi.org/10.1002/qre.2634.

[58] Ouyang M, Dueñas-Osorio L. Time-dependent resilience assessment and improvement of urban infrastructure systems. Chaos: Interdiscipl J Nonlinear Sci Sep. 2012;22(3):033122. https://doi.org/10.1063/1.4737204.

[59] Bruneau M, et al. A framework to quantitatively assess and enhance the seismic resilience of communities. In: Earthquake Spectra. 19. Earthquake Engineering Research Institute; 2003. p. 733–52. https://doi.org/10.1193/1.1623497. no. 4.

[60] Blagojević N, Hefti F, Henken J, Didier M, Stojadinović B. Quantifying disaster resilience of a community with interdependent civil infrastructure systems. Struct Infrastruct Eng 2022. https://doi.org/10.1080/15732479.2022.2052912.

[61] Didier M, Broccardo M, Esposito S, Stojadinovic B. A compositional demand/ supply framework to quantify the resilience of civil infrastructure systems (re-CoDeS) Apr. 2017;3(2):86–102. https://doi.org/10.1080/23789689.2017.1364560.

[62] Fang YP, Zio E. An adaptive robust framework for the optimization of the resilience of interdependent infrastructures under natural hazards. Eur J Oper Res Aug. 2019; 276(3):1119–36. https://doi.org/10.1016/j.ejor.2019.01.052.

[63] Wang J, Zuo W, Rhode-Barbarigos L, Lu X, Wang J, Lin Y. Literature review on modeling and simulation of energy infrastructures from a resilience perspective. In: Reliability Engineering and System Safety. 183. Elsevier Ltd; Mar. 01, 2019. p. 360–73. https://doi.org/10.1016/j.ress.2018.11.029.

[64] NIST. Community resilience planning guide for buildings and infrastructure systems: volume I. Gaithersburg, MD. Oct. 2015. https://doi.org/10.6028/NIST.SP.1190v1.

[65] Kong J, Simonovic SP, Zhang C. Sequential hazards resilience of interdependent infrastructure system: a case study of greater Toronto area energy infrastructure system. Risk Anal May 2019;39(5):1141–68. https://doi.org/10.1111/risa.13222.

[66] Lee EE, Mitchell JE, Wallace WA. Restoration of services in interdependent infrastructure systems: a network flows approach. IEEE Trans Syst Man Cybernet Part C: Appl Rev Nov. 2007;37(6):1303–17. https://doi.org/10.1109/TSMCC.2007.905859.

[67] Haimes YY, et al. Inoperability input-output model for interdependent infrastructure sectors. I: Theory and methodology. 2023. https://doi.org/10.1061/ASCE1076-0342200511:267.

[68] Carreras BA, Lynch VE, Dobson I, Newman DE. Critical points and transitions in an electric power transmission model for cascading failure blackouts. Chaos 2002;12 (4):985–94. https://doi.org/10.1063/1.1505810.

[69] Kinney R, Crucitti P, Albert R, Latora V. Modeling cascading failures in the north American power grid. Europ Phys J B Jul. 2005;46(1):101–7. https://doi.org/10.1140/epjb/e2005-00237-9.

[70] Ouyang M. A mathematical framework to optimize resilience of interdependent critical infrastructure systems under spatially localized attacks. Eur J Oper Res Nov. 2017;262(3):1072–84. https://doi.org/10.1016/j.ejor.2017.04.022.

[71] Nurre SG, Cavdaroglu B, Mitchell JE, Sharkey TC, Wallace WA. Restoring infrastructure systems: an integrated network design and scheduling (INDS) problem. Eur J Oper Res Dec. 2012;223(3):794–806. https://doi.org/10.1016/j.ejor.2012.07.010.

[72] Ouyang M, Fang Y. A mathematical framework to optimize critical infrastructure resilience against intentional attacks. Comput Aided Civ Inf Eng 2017;32(11): 909–29. https://doi.org/10.1111/mice.12252.

[73] IBM ILOG. IBM ILOG CPLEX 12.10 user's manual. IBM ILOG; 2019.

[74] González AD, Dueñas-Osorio L, Sánchez-Silva M, Medaglia AL. The interdependent network design problem for optimal infrastructure system restoration. Comput Aided Civ Inf Eng May 2016;31(5):334–50. https://doi.org/10.1111/mice.12171.

[75] Zhang W, Lin P, Wang N, Nicholson C, Xue X. Probabilistic prediction of postdisaster functionality loss of community building portfolios considering utility disruptions. J Struct Eng Apr. 2018;144(4). https://doi.org/10.1061/(asce)st.1943-541x.0001984.

[76] Adachi T, Ellingwood BR. Serviceability assessment of a municipal water system under spatially correlated seismic intensities. Comput Aided Civ Inf Eng 2009;24 (4):237–48. https://doi.org/10.1111/j.1467-8667.2008.00583.x.

[77] González AD, Dueñas-Osorio L, Sánchez-Silva M, Medaglia AL. The interdependent network design problem for optimal infrastructure system restoration. Comput Aided Civ Inf Eng May 2016;31(5):334–50. https://doi.org/10.1111/mice.12171.